Chapter 35. HYDROGRAPHY AND CIRCULATION OF THE ANTARCTIC CONTINENTAL SHELF: 150°E TO THE GREENWICH MERIDIAN

COASTAL SEGMENT (32,P)

EILEEN E. HOFMANN AND JOHN M. KLINCK

Center for Coastal Physical Oceanography, Old Dominion University

Contents

1. Introduction

The Belgian *Belgica* (1897–1899) expedition and the German *Valdivia* (1898–1899) expedition provided the first hydrographic observations of the waters overlying the Antarctic continental shelf. Following these historic cruises, numerous scientific expeditions took place in specific regions of the Antarctic in the early part of this century (Fogg, 1992). Hydrographic observations from the German *Meteor* expeditions (1925–1927) in the South Atlantic revealed most of the major water masses in the Antarctic. However, the primary effort in describing the hydrographic properties of Antarctic waters came from observations made during the *Discovery* investigations, which provided descriptions of the large-scale (Deacon, 1937) as well as regional (e.g., Clowes, 1934) water-mass distributions.

Existing descriptions of the hydrographic properties and circulation of the extensive continental shelf surrounding the Antarctic continent are limited, and little comparison among regions has been done. The few regional hydrographic analyses are

The Sea, Volume 11, edited by Allan R. Robinson and Kenneth H. Brink
ISBN 0-471-11545-2

based on observations from limited surveys, often done as part of larger programs such as the International Southern Ocean Studies (ISOS) program, which focused on processes controlling the transport of the Antarctic Circumpolar Current (ACC) at Drake Passage (Neal and Nowlin, 1979). Similarly, studies of the Weddell Sea continental shelf resulted from programs such as the International Weddell Sea Oceanographic Expedition (IWSOE), which were designed to understand bottom-water formation processes (e.g., Foster and Carmack, 1976). Knowledge of the hydrographic conditions and circulation on the continental shelf in the Ross Sea resulted from research efforts that focused primarily on interactions between the ice shelves and the ocean (e.g., MacAyeal, 1985).

The development of commerical fisheries in the Southern Ocean in the late 1960s–early 1970s stimulated interest in understanding Antarctic coastal systems so that proper management and conservation measures for Antarctic marine living resources could be established. In 1977, the Biological Investigations of Marine Antarctic Systems and Stocks (BIOMASS) Program (El-Sayed, 1994) was undertaken, which focused on the Antarctic Peninsula and Prydz Bay regions. The physical oceanography component of the BIOMASS program was limited, but it contributed significantly to the otherwise sparse database of hydrographic observations for Antarctic coastal waters. Hence there have been few programs designed specifically to study the hydrography and circulation of the Antarctic continental shelf. Moreover, the majority of the available data are from observations made since the mid-1970s and are from the austral summer.

The limited data show that the Antarctic continental shelf includes regions of bottom water and ice formation and export. Moreover, the Antarctic continental shelf is biologically productive, supporting large populations of whales, seals, penguins, and Antarctic krill (*Euphausia superba*). Thus the potential effects of climate change, developing fisheries, and human-induced changes, such as oil spills, make it appropriate to review what is known of the hydrography and circulation of these regions. Thus the objective of this chapter is to synthesize existing hydrographic and circulation observations for the portion of the Antarctic continental shelf from 150°E eastward to the Greenwich Meridian (Fig. 35.1). This synthesis is based on a review of descriptions from the literature and an analysis of historical hydrographic observations obtained from the U.S. National Oceanographic Data Center (NODC). The NODC data set includes the Southern Ocean hydrographic data compiled by Gordon and Molinelli (1982), as well as that in the more recent atlas by Olbers et al. (1992).

In the next two sections we describe the continental shelf regions and the data sets used in this analysis. This is followed by an analysis of the water mass characteristics and circulation in these regions. The observed distributions and patterns are then compared with those derived from theoretical circulation modeling studies. The final sections provide simple oxygen, salt and heat budgets, as well as a discussion and summary.

2. Environmental Setting

2.1. *Continental Shelf Characteristics*

The continental shelf from 150°E eastward to the Greenwich Meridian encompasses an area of 3.32×10^6 km^2. Over most of this range, the shelf is 200–700 m deep

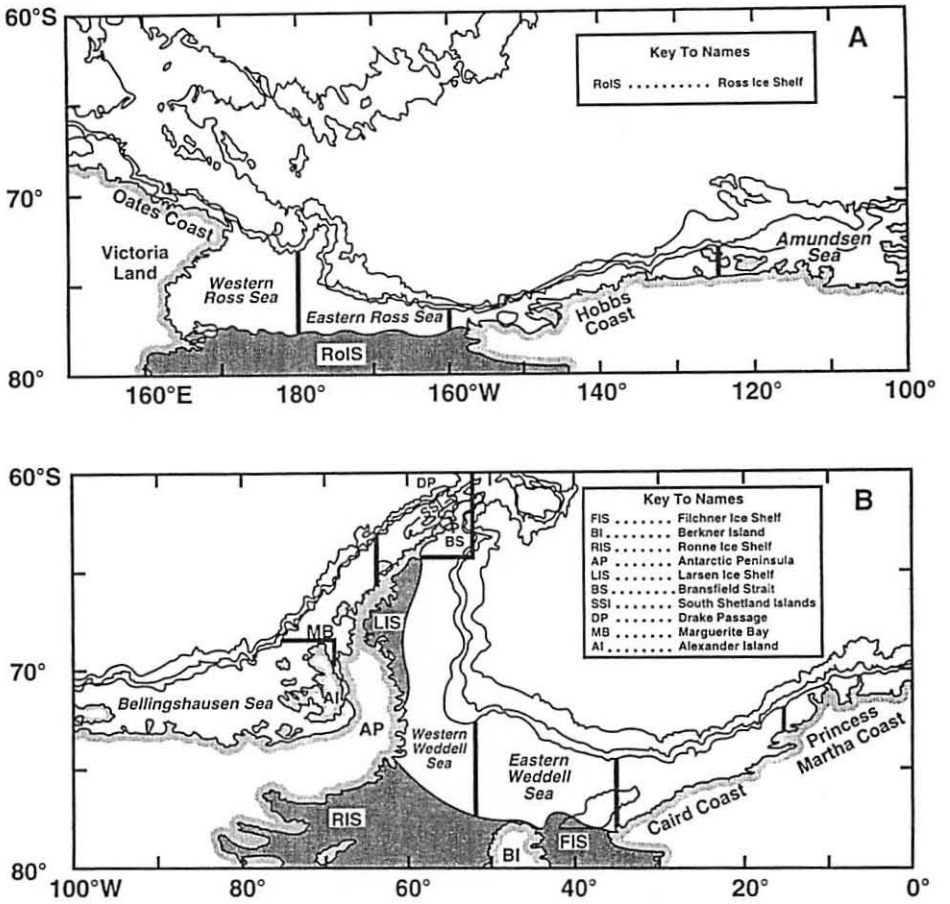

Fig. 35.1. Map showing the Antarctic continental shelf region between (*A*) 150°E to 100°W and (*B*) 100°W to the Greenwich Meridian that was included in the analysis. The heavy lines indicate the 12 subregions for which the temperature–salinity diagrams shown in Figs. 35.4 and 35.5 were constructed. Bathymetry contours represent the 750-, 1500- and 3000-m isobaths.

and is characterized by shallow plateaus, deep holes, and across-shelf trenches. An additional feaure of the Antarctic continental shelf is that it deepens onshore. This structure and the overall rugged topography of the continental shelf results from geological processes, such as ice scour, that formed the shelf. The deeper inshore shelf and the presence of islands in some regions potentially restrict exchanges between nearshore and offshore regions. Beyond the outer edge, the continental shelf deepens rapidly toward the open ocean. The boundary between the continental shelf and offshore slope region varies with location; however, for this analysis, the 750-m isobath was used to define the offshore edge of the continental shelf. This is deep enough to include the continental shelf regions but not so deep as to include offshore slope regions.

The most prominent interruption of the continental shelf between 150°E and the Greenwich Meridian is Bransfield Strait, which is at the northern end of the Antarc-

tic Peninsula (Fig. 35.1*B*). The northern and southern boundaries of Bransfield Strait are formed by the South Shetland Islands and the Antarctic Peninsula, respectively. The western end of Bransfield Strait is bounded by a shallow sill that is 200–500 m deep; the eastern end is open toward the Weddell Sea. The shelf to the north of the South Shetland Islands is interrupted by two narrow trenches, which provide the only deep connections between Bransfield Strait and Drake Passage. The only deep connection between Bransfield Strait and the west Antarctic Peninsula continental shelf is through the narrow Gerlache Strait. Hence exchange of Bransfield Strait waters with oceanic waters to the north and shelf waters to the west is limited to the upper 200–500 m. Exchanges with the Weddell Sea to the east can occur throughout most of the water column.

2.2. *Wind Patterns*

Wind stress is one of the major forces affecting circulation in the Southern Ocean. Direct observations of wind direction and speed are limited due to the small number of meteorological stations south of 45°S (Bromwich and Stearns, 1993). However, wind stress climatologies are available for the global ocean, which are based on ship observations (e.g., Hellerman and Rosenstein, 1983) or global atmospheric forecast models, such as the forecasts provided by the European Centre for Medium Range Weather Forecasting (ECMWF; Trenberth et al., 1989). Either approach for obtaining a wind stress climatology involves assumptions, and for the Southern Ocean, some of these can be questionable. A recent analysis (Chelton et al., 1990) indicates that the Trenberth et al. (1989) climatology may be most representative of wind stress for the Southern Ocean.

The Trenberth et al. (1989) wind climatology, which extends to only 70°S, illustrates the general structure and seasonal variation of the wind stress between 180° and the Greenwich Meridian (Fig. 35.2). The annual average wind stress is primarily from the north–northwest over the entire region. Partitioning the wind stress variance into annual and semiannual components (Trenberth et al., 1990, Figs. 6, 7) shows that the zonal component of wind stress has a significant (more than 60% of the total variance) annual variation, while the meridional component has a significant semiannual variation. The semiannual variation in wind stress is such that the weakest stress occurs during austral summer and the strongest during austral winter. In general, the wind strength changes by a factor of 2 or more with little variation in wind direction. The semiannual change in wind speed over the Southern Ocean has been attributed to the latitudinal difference in the timing of seasonal heating of the atmosphere south of 35°S (van Loon, 1967; van Loon and Rogers, 1984a,b), which creates two maxima in the atmospheric meridional surface pressure gradient. Direct measurement of atmospheric pressure and surface winds made during the First GARP Global Experiment (FGGE) from a large number of free-drifting surface buoys in the Southern Ocean (Large and van Loon, 1989) verified the existence of a semiannual variation in atmospheric conditions over the ocean south of 60°S.

In the continental shelf regions that are included in the wind climatology, such as the Antarctic Peninsula, the general wind direction is primarily from the north–northeast (Fig. 35.2), which produces a downwelling circulation over the continental shelf and a southward flow along the coast. This, combined with the northward flow of the Antarctic Circumpolar Current (ACC) at the outer shelf edge, would result

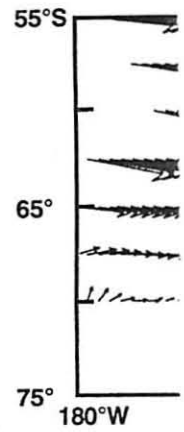

Fig. 35.2. Annua
Meridian estimatec
stress is indicated

in a cyclonic c
nism. The aver
exists over the

The wind st
an atmospheric
represent the A
continent and p
numerous islan
the wind field o
in the large-scal
automatic weat

Sea ice cover in
to 20×10^6 kn
to the edge of t
fluxes between
potentially hav

The average
average of brig
multichannel r
tration (Gloers
ary (Fig. 35.3*A*
Coast, from th
edge of the We
fringe along th
the western We
near the coast,

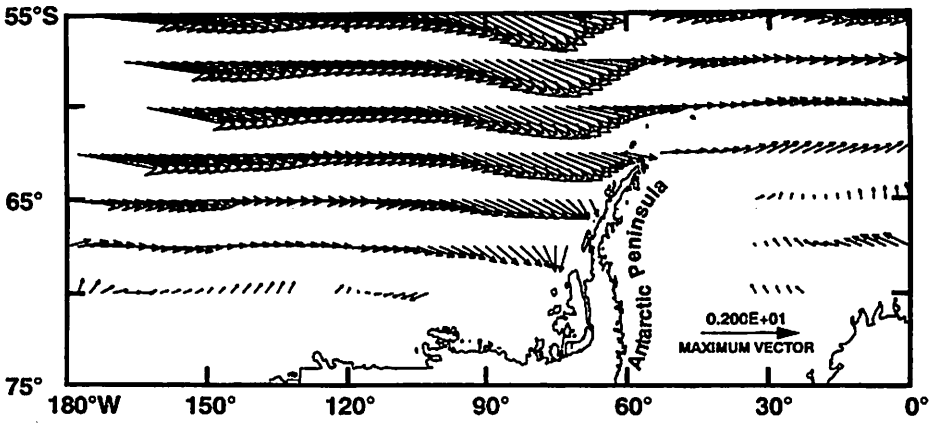

Fig. 35.2. Annual mean wind stress (dyn cm^{-2}) between 55 and 75°S and 180°W and the Greenwich Meridian estimated from the ECMWF global atmospheric forecast model. The magnitude of the wind stress is indicated by the length of the vectors. (Data from Trenberth et al., 1989.)

in a cyclonic circulation over the shelf in the absence of any other forcing mechanism. The average annual wind stress suggests that cyclonic atmospheric circulation exists over the Weddell Sea.

The wind stress estimates provided by Trenberth et al. (1990) are produced from an atmospheric model with a grid spacing of 2.5°, which is too coarse to properly represent the Antarctic land topography. The tall mountain chains along the Antarctic continent and peninsula, along with topographic steering by nearshore channels and numerous islands, as well as katabatic winds off the continent, create local changes in the wind field on scales of tens of kilometers. However, the general patterns observed in the large-scale fields are consistent with those seen in wind records from land-based automatic weather stations (Bromwich and Stearns, 1993).

2.3. *Sea Ice*

Sea ice cover in the Southern Ocean ranges from 4×10^6 km^2 in the austral summer to 20×10^6 km^2 in the austral winter. In the summer, the ice edge retreats almost to the edge of the Antarctic continent. Thus heat, fresh water (salt) and momentum fluxes between the ocean and atmosphere over the Antarctic continental shelf regions potentially have strong seasonal components.

The average monthly sea ice concentration for the Antarctic, based on a nine-year average of brightness temperature measurements from the polar-orbiting, scanning multichannel microwave radiometer (SSMR) which are converted into ice concentration (Gloersen et al., 1992), show that the minimum ice cover is during February (Fig. 35.3*A*). At this time, ice cover greater than 60% is found along the Oates Coast, from the eastern Ross Sea to the Bellingshausen Sea, and along the western edge of the Weddell Sea. The Ross Sea is ice-free in February, except for a narrow fringe along the southern and western edges. The southern Bellingshausen Sea and the western Weddell Sea are covered with ice concentrations above 90%. However, near the coast, between 135°W and the southern Bellinghausen Sea, there are regions

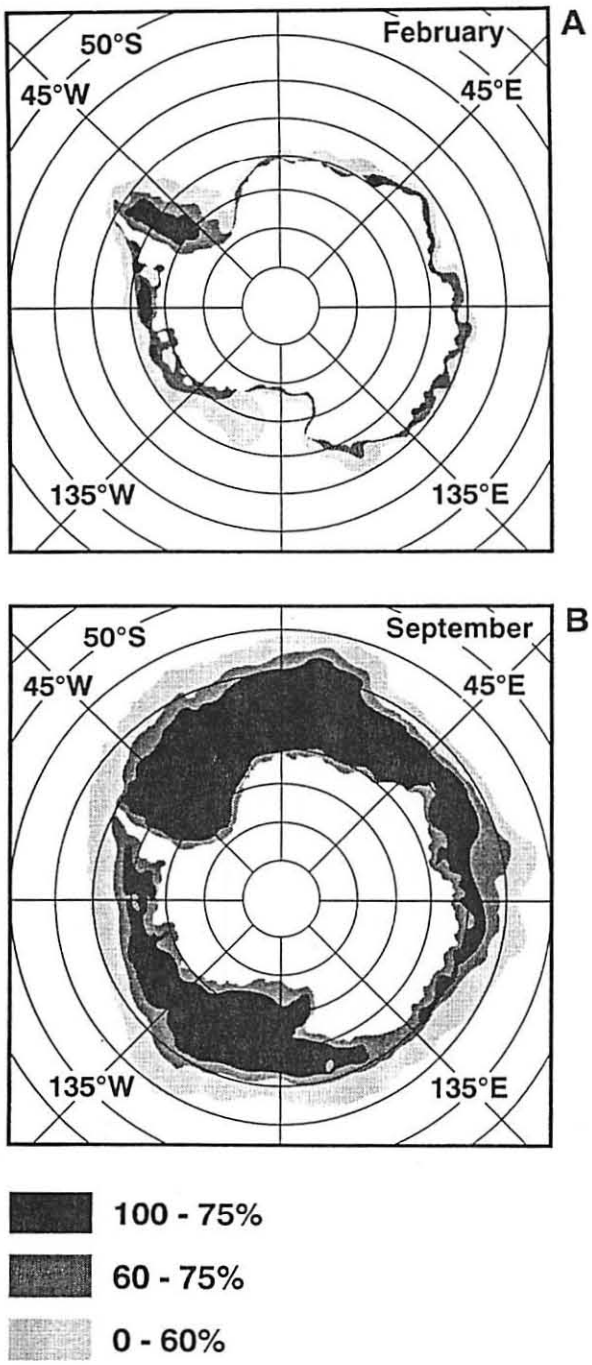

Fig. 35.3. Percent ice cover around the Antarctic continent in (*A*) February and (*B*) September. (Adapted from Gloersen et al., 1992.)

of reduced ice cover. The western and northern coasts of the Antarctic Peninsula are covered by pack ice with concentrations up to 60%.

Maximum sea ice cover occurs during September (Fig. 35.3*B*), although the maximum in ice thickness (more areas have nearly 100% cover) is in August. The ice thickness measurements indicate that around the entire continent, ice concentrations are larger offshore and thinner within 50 km of land along the coast. Along the tip of the Antarctic Peninsula, the ice is thinner, with a clear pattern of reduction in ice concentration from southwest to northeast.

The climatologies presented in Gloersen et al. (1992) show that by November sea ice concentrations are strongly reduced from the winter maximum. In the interior Ross Sea, an area of low ice concentration forms, which turns into a large open area in December. By January, the Ross Sea is open to the north; thus ice retreat in the Ross Sea begins in the interior, rather than a uniform retreat of the ice edge to the south. The eastern Weddell Sea also melts quickly from December to January. Low sea ice concentration is centered over Maud Rise near the Greenwich Meridian in December. By January, the eastern half of the gyre is ice-free, and the ice continues to retreat westward, reaching a minimum in February.

The Bellingshausen Sea develops sea ice in June. By July the continental shelf around the Antarctic Peninsula is ice covered, with concentrations above 50% (Gloersen et al., 1992). The ice retreat starts in September, but ice concentration in the southern Bellingshausen Sea increases from November to January, indicating that the ice is being compressed from the north in addition to melting. Ice in the Bellingshausen Sea is still melting in February at a time when the eastern Ross Sea is beginning to freeze. Throughout the period of reduction in ice concentration, the southern Bellingshausen Sea changes very little.

In August, the sea ice cover along the tip of the Antarctic Peninsula begins to decrease at a time when other areas are still covered with ice. Also, ice formation in this region begins in April and continues until June, when other coastal areas are completely covered with heavy ice.

The patterns in sea ice cover obtained from the climatologies presented in Gloersen et al. (1992) represent average conditions. Recent studies (Fraser et al., 1992; Murphy et al., 1995) have shown a cyclic pattern in the extent and duration of Antarctic sea ice cover, with periods of extensive ice coverage occurring about every four to six years. Moreover, the occurrence of high- or low-ice years is not coherent around the Antarctic continent (Stammerjohn, 1993), but rather the signal in sea-ice extent precesses around the Antarctic continent with a period of approximately seven to nine years (Murphy et al., 1995). This spatial variability in the extent of ice cover has been linked to anomalies in surface pressure, wind and sea-surface temperature, which propagate eastward with the circumpolar flow with a period of four to five years and take about eight to 10 years to encircle the pole (White and Peterson, 1996).

2.4. Coastal Polynyas

Important features of the Antarctic and Arctic coastal areas are polynyas, which are regions of open water that occur even when atmospheric conditions are such that the surface water should freeze. Polynyas are typically rectangular or elliptical in shape with dimensions that range from a few kilometers to hundreds of kilometers. Polynyas differ from leads, which are narrower but can be many kilometers in length. The

mechanisms that create leads and polynyas are different and are discussed in Smith et al. (1990). However, polynyas and leads have the same effect, in that they allow large heat fluxes between the ocean and atmosphere (up to 100 times larger than the flux through the ice) and are sites of large salinity fluxes due to brine rejection during freezing.

Polynyas exist in one of two major forms, latent heat or sensible heat polynyas (Zwally et al., 1985), which are differentiated by the source of heat to the atmosphere. A sensible heat polynya is kept ice-free by continued upwelling of warm water from deep in the ocean. Water above 0°C [e.g., Circumpolar Deep Water (CDW), discussed in Section 4.1] is capable of keeping an area ice-free if it is supplied at a sufficient rate. Sensible heat polynyas tend to appear in the same location, which argues that the geometry of the bottom or nearby coast has a strong influence on upwelling of the warmer water. In contrast, latent heat polynyas are kept ice-free by the mechanical removal of ice by wind-driven transport. In this case the water near the surface is at the freezing point and frazil ice is actively forming, but it is removed before having a chance to consolidate into a solid sheet. Even though the ocean temperature does not change, considerable heat (latent heat of fusion of ice) is liberated to the atmosphere. A by-product of this continued production of sea ice is the creation of considerable amounts of brine which sink into the mixed layer, causing an increase in salinity. In general, polynyas on high-latitude continental shelves are latent heat polynyas, whereas those in the open ocean are sensible heat polynyas. However, some counterexamples exist and some polynyas have both sensible and latent heat processes active.

A combination of two processes is required to create a latent heat polynya (Kurtz and Bromwich 1985): offshore transport of newly formed sea ice and blockage of transport of existing ice into the open area. If the winds diminish, water freezes to create a solid ice cover. As the winds increase, the thin ice cover can be broken up and exported (Kurtz and Bromwich, 1985). Such conditions exist in polynyas in Terra Nova Bay (164°E, 75°S) on the Ross Sea (Bromwich and Kurtz, 1984; Kurtz and Bromwich, 1985) and St. Lawrence Island in the Bering Sea (Schumacher et al., 1983), among other examples. In the Terra Nova Bay polynya, an ice tongue projects from the coast on the south side of the Bay, blocking the approach of existing sea ice. The St. Lawrence Island polynya is on the south side of an east–west elongated island that blocks ice that is driven south by the polynya-creating northerly winds.

Observational studies of coastal polynyas in the Arctic and Antarctic provide insight into how these features form, the frequency at which they form, and their spatial extent. Time-series observations over 230 days revealed 11 events of northerly winds which created open water on the south side of St. Lawrence Island (Schumacher et al., 1983). During these times, the air temperature dropped, water cooled to the freezing point and the salinity increased. The water in the polynya was shallow (20–40 m) and the polynya openings were short-lived (65 h on average), but the salinity increased by as much as 0.008 h^{-1}. The estimated heat loss was 535 W m^{-2}.

The polynya in Terra Nova Bay (western Ross Sea) recurs every winter (Bromwich and Kurtz, 1984; Kurtz and Bromwich, 1985) and covers an average area of 1300 km^2. Katabatic winds (15–20 m s^{-1}) occur over this bay due to dense (cold) air from the Antarctic continent flowing down glacial valleys. These strong winds blow offshore, taking the newly formed ice with it. Atmospheric heating occurs due to 400–600 W m^2 of sensible heat flux and 175–200 W m^2 of latent heat flux. This heat

comes from seawater freezing at the ocean surface, which is estimated to occur at rates of 0.2 m day^{-1}. High-Salinity Shelf Water (discussed in Section 4.1) is observed in this polynya, and it becomes saltier by the interaction with the polynya.

Passive microwave observations spanning 1979–1986 were used to analyze ice cover for the Ross Sea (Jacobs and Comiso, 1989). Oceanographic studies in 1984 allowed comparison of satellite and in situ measurements. Two polynyas were analyzed: the Ross Ice Shelf polynya, which was a latent heat polynya, and a northwest shelf polynya, which was a sensible heat polynya. The Ross Ice Shelf polynya was correlated with synoptic southerly wind events which moved ice away from the ice shelf. creating open water. This large area of open water delayed the formation of ice in the succeeding fall, due to increased heat storage from solar insolation and reduced albedo. Breakup of sea ice in summer was also enhanced in these regions, due to open water. The sensible heat polynya on the northwest shelf was associated with upwelling of CDW (discussed in Section 4.1) near a shallow bank, which provided heat to melt the ice cover. As mentioned in the preceding section, this region is known for its early breakup of winter ice cover.

During a three-month period in 1979, six polynyas were observed to open off Wilkes Land (90 to 150°E), which were strongly correlated with synoptic wind events (Cavalieri and Martin, 1985). These polynyas, which were open for a total time of 100 days, resulted in heat fluxes of 50 to 800 W m^{-2} and salinity increases between 0.3 and 0.7.

A persistent polynya near Cape Ann (52°E) was observed (Comiso and Gordon, 1996) to recur every winter with intervals of a few days to a few weeks. Two formation mechanisms were identified. Synoptic storms remove ice from this region, creating open water that persisted for many days. A coastal polynya is observed just off Cape Ann, which is driven by upwelling of warmer water by a constriction of the flow by the cape. This feature appears to be stable due to the influx of warmer water and is thus a sensible heat polynya. The location is stable due to the bathymetric effect on the upwelling.

A detailed study of ice conditions in the southern Weddell Sea (Eicken and Lange, 1989) revealed numerous latent heat polynyas which were related to offshore wind stress and tended to develop in the lee of coastal promontories. Winds were observed to be easterly and northeasterly (the orientation of the coastline is northeast-southwest), with air temperatures as low as −15°C. These polynyas were tens to hundreds of kilometers in length (along the coast) and up to 30 km wide. The type of sea ice created depended on the wind speed, with weak winds (<3 m s^{-1}) allowing columnar ice to form, medium winds (3–10 m s^{-1}) producing rafted and ridged ice with mixed granular and columnar composition, and strong winds (>10 m s^{-1}) producing granular ice with considerable rafting and ridging.

Passive microwave observations from satellites which have been available since 1974 were used to study 16 coastal polynyas spread evenly around the Antarctic continent (Zwally et al., 1985). The fraction of open water in the satellite observations was used to identify the size of transient polynyas. This study also provides a discussion of polynya formation processes and gives the first categorization of polynyas by heat source (latent and sensible). Polynyas were shown to increase the open-water fraction of local ice cover in different regions by 7–32% and to lead to an increase in ocean salinity of 0.22–0.347, which is sufficient to increase the salinity of deep water to allow for formation of Antarctic Bottom Water.

3. Hydrographic Data

Hydrographic data for the continental shelf between 150°E eastward to the Greenwich Meridian for depths less than 750 m were obtained from the NODC *World Ocean Atlas* (Levitus and Boyer, 1994a,b; Levitus et al., 1994). These data consist of the original hydrographic observations, the observations interpolated to standard depths and observations objectively interpolated to a 1° grid. All of the analyses presented in this study used the original observations of in situ temperature, salinity and dissolved oxygen from original depths. The *World Ocean Atlas* data have undergone extensive quality control procedures and only those values flagged by NODC as good were used. Additional quality control for this analysis consisted of checking property value ranges and visual inspection of property–property plots and vertical profiles.

The area of interest (Fig. 35.1) is extensive, therefore, to facilitate comparisons, five regions and 12 subregions were defined (Table I, Fig. 35.1). The five larger regions include the Antarctic Peninsula, the Bellingshausen Sea, the Amundsen Sea and two gyre circulations: the Ross Sea and the Weddell Sea. Within each region, hydrographic properties may vary, such as on the eastern and western sides of gyres. Consequently, the regions were subdivided on the basis of geographic or bathymetric features that may influence hydrographic distributions or circulation patterns.

Temperature and salinity observations for the Antarctic continental shelf between 150°E and the Greenwich Meridian are concentrated in the Ross Sea and west of the Antarctic Peninsula (Table I). These areas have been the subject of several national and international programs and are the regions where several nations maintain shore-

TABLE I
Summary of the Region and Subregion Definitions and the Number of Hydrographic Stations That Are Available in Each for Construction of Temperature–Salinity and Temperature–Oxygen Diagrams

Area	Latitude (°S)	Longitude (°E or °W)	T–S Stations (number)	T–O_2 Stations (number)
Large Regions				
Ross Sea	80–60	150–160	1207	264
Amundsen Sea	80–70	160–100	47	18
Bellingshausen Sea	80–71	100–70	29	17
Antarctic Peninsula	71–60	80–60	702	176
Weddell Sea	80–60	60–0	308	301
Subregions				
Oates coast	71–65	150–170	15	
Western Ross Sea	80–71	160–180	667	
Eastern Ross Sea	80–70	180–160	525	
Hobbs coast	80–70	160–125	41	
Amundsen Sea	75–70	125–100	6	
Bellingshausen Sea	75–69	100-70	29	
Antarctic Peninsula	69–62	75–64	112	
Bransfield Strait	65–60	64–54	590	
Western Weddell Sea	80–65	64–52	27	
Eastern Weddell Sea	80–70	52–35	113	
Caird coast	80–70	35–15	137	
Princess Martha coast	75–65	15–0	31	

based research facilities. The nearly permanent sea ice cover in the western Weddell Sea limits the majority of the available temperature and salinity data to the southern continental shelf. The limited temperature and salinity observations on the continental shelf in the Amundsen and Bellingshausen Seas result from only four to six cruises, all of which occurred in the austral summer. Within all subregions, including the Amundsen Sea, the observations are sufficient to construct temperature–salinity diagrams. Dissolved oxygen measurements are considerably fewer (Table I); therefore, temperature–oxygen diagrams were constructed for only the larger regions.

4. Water Mass Properties and Distribution

4.1. General T–S Properties

The in situ temperature–salinity (T–S) diagrams constructed for the 12 subregions (Figs. 35.4 and 35.5) show that salinity ranges from about 33.0 to 35.0 and temperature ranges from −2.0°C to slightly greater than 2°C. The range of temperature and salinity values seen in the upper 100 m illustrates the variability in water properties that is produced by seasonal processes such as sea ice melting and freezing, solar heating, wind mixing and the development and decay of upper water column stratification. The largest variability in temperature and saliniy in the upper 100 m is in the Antarctic Peninsula and Bransfield Strait regions (Fig. 35.5*A*,*B*). Below 100 m, the scatter in T–S space is reduced and salinities remain above 34.0 in most regions.

A distinct feature in all subregion T–S diagrams is a cluster of points at salinities of 34–34.4 and temperatures of 0.0 to −2.0°C. This defines Antarctic Surface Water (AASW), which is attributed to winter cooling (Mosby, 1934; Gordon et al., 1977; Toole, 1981). During the winter, the entire upper water column is composed of AASW. During the summer, increased solar insolation warms the surface waters and isolates a core of AASW that appears as a distinct temperature minimum around 100 m at the outer edge of the continental shelf, which then shallows onshore (Toole, 1981). This feature has been referred to as Winter Water (Mosby, 1934; Sievers and Nowlin, 1984), and it is the part of AASW that undergoes minimal seasonal modification.

Another prominent feature in the T–S diagrams is CDW, which is characterized by a salinity maximum (salinities up to 34.73) and a temperature maximum ($T >$ 0°C). CDW is the most voluminous water mass transported by the ACC (Sievers and Nowlin, 1984), and its presence in Antarctic coastal regions was noted by Deacon (1937) and Gordon (1967). This water mass is found in all subregions except the western and eastern Weddell Sea (Fig. 35.5*C*,*D*) regions. In the Antarctic Peninsula and Bransfield Strait subregions (Fig. 35.5*A*,*B*), CDW divides into two branches, Upper CDW (UCDW) and Lower CDW (LCDW), which reflect different properties acquired in different source regions (Gordon, 1967). South of the Subantarctic Front, UCDW is characterized by a maximum in temperature that arises from the overlying Antarctic Intermediate Water and Winter Water (Whitworth and Nowlin, 1987). This water mass is further characterized by an oxygen minimum and nutrient maxima whose sources are in the Indian and Pacific Oceans (Callahan, 1972). The LCDW is characterized by a salinity maxima that is derived from North Atlantic Deep Water (Gordon, 1967; Reid et al., 1977; Whitworth and Nowlin, 1987) and by a nitrate minimum (Sievers and Nowlin, 1984; Whitworth and Nowlin, 1987). The characteristics of these water masses are summarized in Table II.

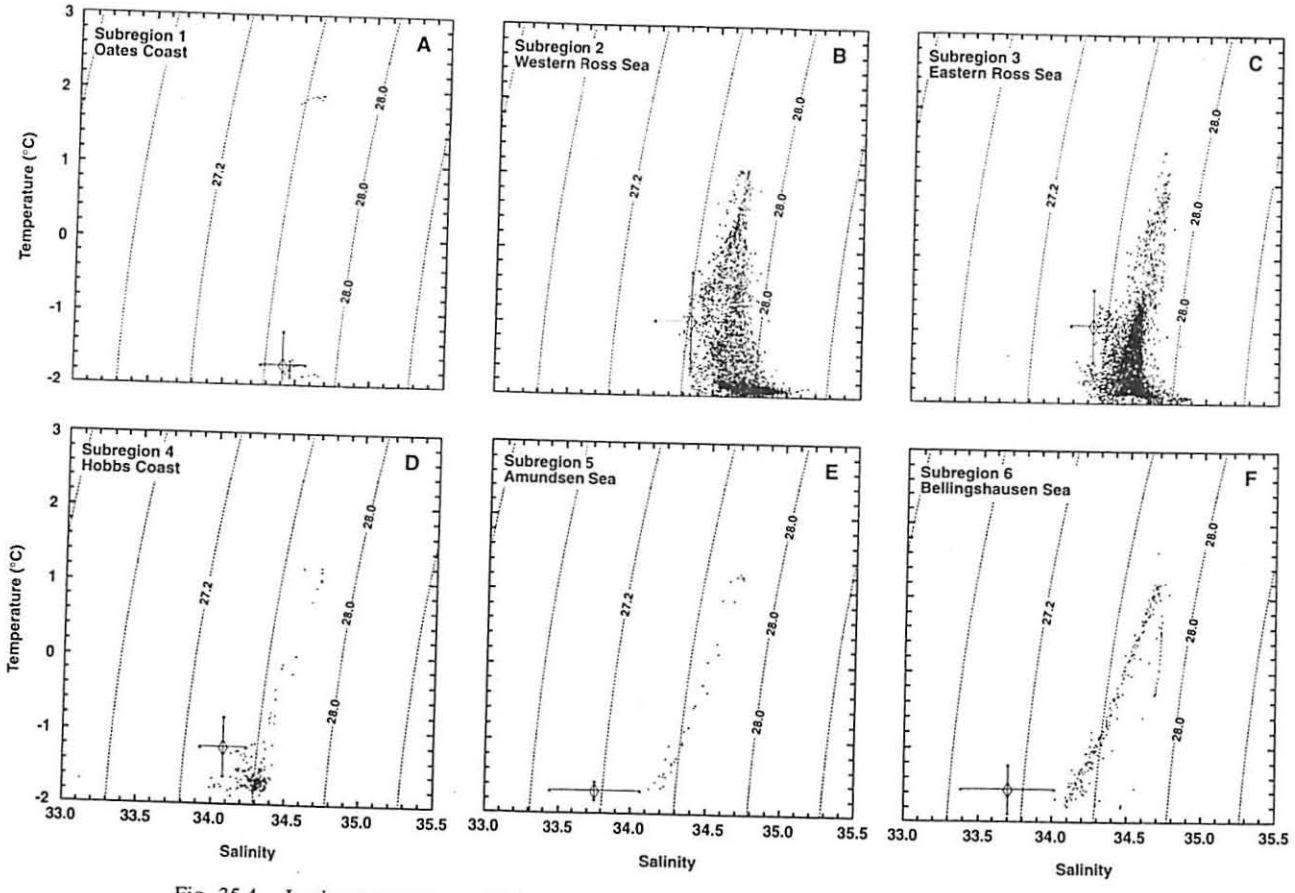

Fig. 35.4. In situ temperature–salinity diagrams constructed from the NODC hydrographic data set using observations below 100 m for (*A*) Oates coast, (*B*) Western Ross Sea, (*C*) Eastern Ross Sea, (*D*) Hobbs coast, (*E*) Amundsen Sea and (*F*) Bellingshausen Sea. Subregion boundaries are shown on Fig. 35.1*A*. The solid lines indicate values of 1 standard deviation for temperature and salinity measured above 100 m. The contours represent lines of constant σ_t.

Fig. 35.4. In situ temperature–salinity diagrams constructed from the NODC hydrographic data set using observations below 100 m for (*A*) Oates coast, (*B*) Western Ross Sea, (*C*) Eastern Ross Sea, (*D*) Hobbs coast, (*E*) Amundsen Sea and (*F*) Bellingshausen Sea. Subregion boundaries are shown on Fig. 35.1*A*. The solid lines indicate values of 1 standard deviation for temperature and salinity measured above 100 m. The contours represent lines of constant σ_t.

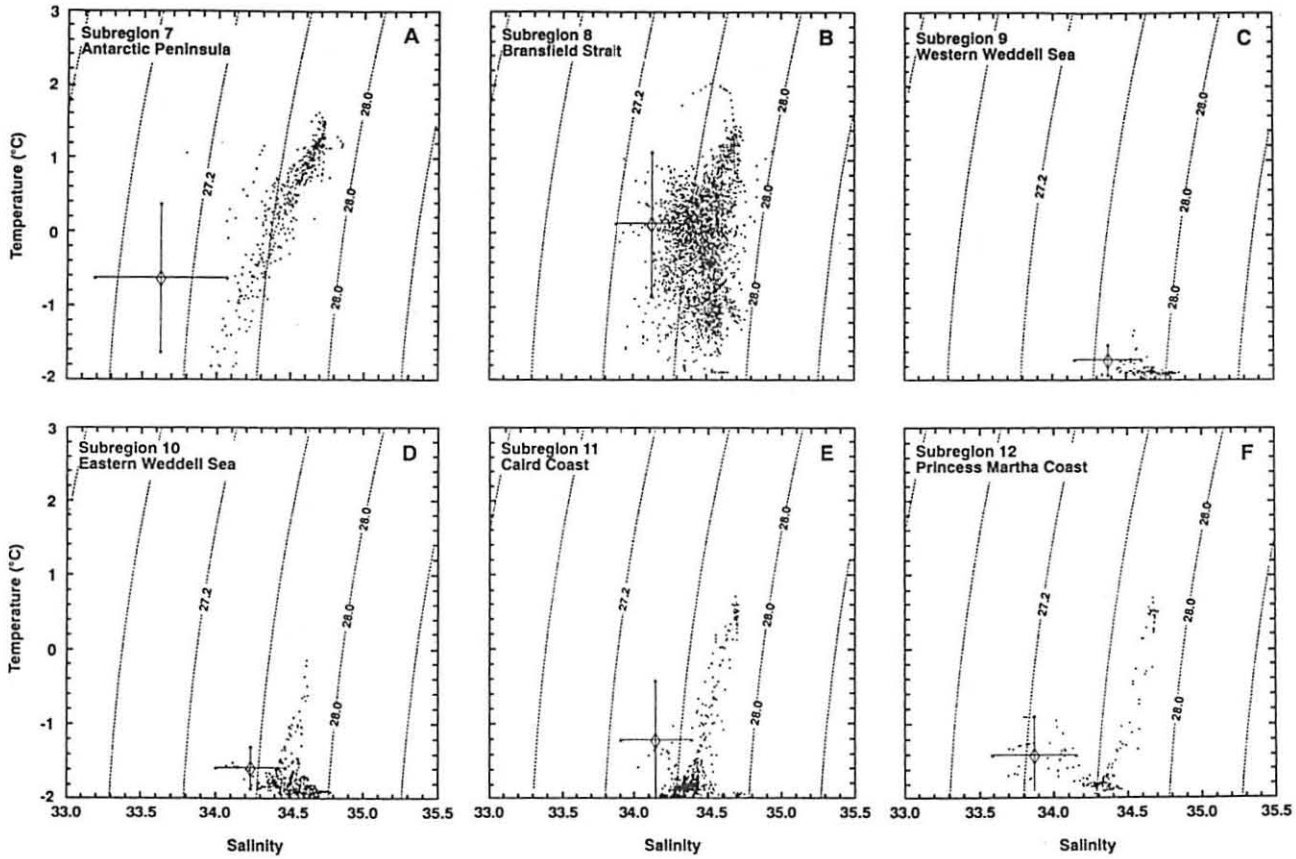

Fig. 35.5. In situ temperature–salinity diagrams constructed from the NODC hydrographic data set using observations below 100 m for (*A*) Antarctic Peninsula, (*B*) Bransfield Strait, (*C*) Western Weddell Sea, (*D*) Eastern Weddell Sea, (*E*) Caird coast and (*F*) Princess Martha coast. Subregion boundaries are shown on Fig. 35.1*B*. The solid lines indicate values of 1 standard deviation for temperature and salinity measured above 100 m. The contours represen lines of constant σ_t.

TABLE II
Summary of the Major Water Masses Found on the Antarctic Continental Shelf between 150°E and the Greenwich Meridian

Water Mass	Temperature (°C)	Salinity	Location[a]
Antarctic Surface Water (AASW)	0.0 to −1.5	34.0–34.4	All regions
Winter Water	<−1.5	34.0–34.4	All regions
Circumpolar Deep Water (CDW)	>0	34.6–34.73	All regions except Weddell Sea
Upper CDW (UDCW)	1.5–2.0	34.6–34.7	AP and BrS
Lower CDW (LCDW)	1.3–1.6	34.7-34.73	AP and BrS
Modified CDW (mCDW)	1.0–1.4	34.6–34.7	All regions except Weddell Sea and Oates coast[b]
Shelf Water	<−1.8	34.2–34.9	Oates coast, Ross and Weddell Seas, Caird coast, Princess Martha coast
High-Salinity Shelf Water (HSSW)	−1.9	34.6–34.9	Ross and Weddell Seas, Caird coast
Low-Salinity Shelf Water (LSSW)	<−1.8	34.4–34.6	Ross and Weddell Seas, Caird coast
Ice Shelf Water			
Shallow Ice Shelf Water (SISW)	<−1.8	34.36–34.42	Ross and Weddell Seas
Deep Ice Shelf Water (DISW)	<−2.0	34.62	Ross and Weddell Seas
Bottom Water			
Low-Salinity Bottom Water (LSBW)	−0.1	34.65	Ross Sea
High-Salinity Bottom Water (HSBW)	0.5	34.71	Ross Sea
Bransfield Strait Water (BS)	<0.0	34.45–34.6	Bransfield Strait
Modified Weddell Deep Water (MWDW)	−1.8 to −0.5	34.45–34.65	Weddell Sea
Western Shelf Water (WSW)	−1.88	34.7–34.85	Weddell Sea
Eastern Shelf Water (ESW)	−1.88	34.29–34.4	Weddell Sea

[a]AP, Antarctic Peninsula; BrS, Bransfield Strait.
[b]Hydrographic data sufficient to determine the presence or absence of the water mass are not available.

All subregions except 1, 9 and 10 (Figs. 35.4*A*; 35.5*C,D*) show an additional water mass that is a cooled form of CDW. The exact characteristics of this modified water depend on the character of CDW at the shelf break (Jacobs et al., 1970; Smith et al., in press). Hence, this modified CDW is designated as mCDW to reflect this regional variability. The apparent lack of modified CDW in the Oates Coast region may be the result of the limited number of hydrographic measurements for this shelf (Table I). The mCDW is reduced in temperature (1.0–1.4°C) and salinity (34.6–34.7) relative to CDW. This water mass forms from a mixture of AASW and CDW (Jacobs et al.,

1970; Smith et al., in press). The tight relationship in the T–S diagams indicates that mCDW retains its integrity as it circulates on the continental shelf.

The cold (<−1.8°C) and salty (34.2–34.9) water mass that occurs in most subregions (Table II) is referred to as Shelf Water (Carmack, 1990), which is then subdivided into more specific water masses. In the Ross and Weddell Seas (Figs. 35.4*B*,*C*; 35.5*C*,*D*) the cold (−1.9°C), salty (up to 34.9) water mass is termed High-Salinity Shelf Water (HSSW) (Table II). A second cold water mass with salinities between 34.4 and 34.6 also occurs and has been termed Low-Salinity Shelf Water (LSSW; Table II). The low temperature and high salinity of HSSW make this the densest water mass in the Antarctic (Jacobs et al., 1985). Carmack (1977) defined HSSW as shelf water with salinity above 34.6, which combined with the cold temperature, results in a water mass that is dense enough to contribute to bottom water formation. The HSSW in the Ross Sea has been referred to as Ross Sea Shelf Water (Jacobs et al., 1970). The large amount of HSSW in the Ross Sea is believed to be formed along the Victoria Land Coast as a result of brine rejection due to sea-surface freezing and glacial meltwater and precipitation (Jacobs et al., 1985). The HSSW in the Weddell Sea, referred to as Western Shelf Water (Carmack, 1977), is less saline than its counterpart in the Ross Sea (Jacobs et al., 1985).

4.2. *Subregion T–S Properties*

The hydrographic observations for the continental shelf waters off the Oates Coast (Fig. 35.4*A*) are limited (Table I); consequently, the full range of the T–S distribution cannot be determined. However, the limited measurements show the presence of AASW and CDW. The outer edge of the continental shelf along this coast is north of 70°S. Hence the temperature maximum of CDW is similar to that observed along the Antarctic Peninsula.

The T–S properties in the western Ross Sea (Fig. 35.4*B*), in contrast, are more complex, with AASW, CDW, mCDW, HSSW and LSSW clearly present. Also, an additional water mass occurs that is characterized by salinities above 34.4 and temperatures that are below the sea-surface freezing point (<−1.8°C). This water mass, termed Ice Shelf Water, is formed from melting beneath the ice shelves. Ice Shelf Water can be subdivided into Shallow Ice Shelf Water (SISW) and Deep Ice Shelf Water (DISW). The former has an average salinity of 34.36–34.42, is typically found at depths of 100 m and extends only a short distance beyond the ice shelves (Jacobs et al., 1985). The average salinity of DISW is about 34.62, and this water mass is found along the bottom and has a large lateral extent, sometimes extending seaward to the shelf break (Jacobs et al., 1985). The final water mass found in the western Ross Sea is Bottom Water, which is characterized by high salinity and cold temperatures (Table II). As with the Ice Shelf Water, this mass is subdivided into Low-Salinity Bottom Water (LSBW) and High-Salinity Bottom Water (HSBW). The latter water mass has been referred to as Ross Sea Bottom Water (Jacobs et al., 1970; Gordon and Tchernia, 1972). LSBW is formed from nearly equal portions of deep (CDW) and shelf waters (Jacobs et al., 1985). The HSBW is also formed from a mixture of deep and shelf waters; however, the contribution from CDW and DISW to this water mass is higher than for LSBW (Jacobs et al., 1985). This water mass is found along the continental slope to the west and north of the Ross Sea. The water mass structure

in the eastern Ross Sea (Fig. 35.4*C*) is similar to the western Ross Sea, except for the reduced presence of HSSW, DISW and Bottom Water.

Hydrographic observations of the continental shelf waters in the Hobbs Coast subregion are limited (Table I), but the station distribution is adequate to provide across-shelf coverage. The water mass structure in this region (Fig. 35.4*D*) is simple relative to that in the Ross Sea, consisting of AASW, CDW and mCDW. Similar water mass structures are seen in the Amundsen Sea (Fig. 35.4*E*) and Bellingshausen Sea (Fig. 35.4*F*) subregions. However, in the Bellingshausen Sea subregion, LCDW is also present. Thus this entire portion of the Antarctic continental shelf lacks the cold, saline water that results in Ice Shelf Water, Bottom Water, HSSW and LSSW.

Between 80 and 75°W, the continental shelf turns northward along the Antarctic Peninsula. The water mass structure of the shelf waters along the southern portion of the Peninsula (Fig. 35.5*A*) is similar to that found to the west in the Bellingshausen Sea, consisting of AASW, CDW and mCDW. However, in this region the two forms of CDW, UCDW and LCDW, can be distinguished.

The *T–S* diagram from the Bransfield Strait subregion (Fig. 35.5*B*) shows more variability than those for the subregions to the west. This subregion also includes a portion of the west Antarctic Peninsula continental shelf. In this subregion, AASW, UCDW, LCDW and mCDW are present. The large scatter in the *T–S* diagram is from Bransfield Strait, where many water types from Drake Passage, the Weddell Sea and the west Antarctic Peninsula shelf come together, thereby producing a complex structure in the upper water column (Stein, 1983, 1986, 1989).

Within Bransfield Strait there is an additional water mass, with temperatures less than 0°C and salinities of 34.45–34.6, which has been referred to as Bransfield Strait water. Gordon and Nowlin (1978) suggested that this water may form locally since the distinct basins in the Bransfield Strait would restrict exchanges at depth. However, Whitworth et al. (1994) argue that the deep waters in Bransfield Strait are a mixture of CDW in the Weddell Sea and the shelf waters from the northwest Weddell Sea. A mixture of this water flows westward north of the Antarctic Peninsula, where it sinks along isopycnals to renew the deep waters of the Bransfield Strait. As indicated by Whitworth et al. (1994), this mixing scheme can occur throughout the year and does not depend on winter convection, which has not been observed in Bransfield Strait. This water is then trapped in the deep basins of Bransfield Strait and consequently has little effect on the deep thermohaline circulation. Above 1000 m, the colder water in the southern portion of the Strait may be partially or wholly derived from inflows from the Weddell Sea.

The *T–S* observations from the western Weddell Sea subregion are primarily from the southwestern corner and are of limited extent. Most of the temperatures are at or below the surface freezing point (Fig. 35.5*C*), and salinity in this subregion is generally high, ranging from 34.2 to almost 34.9. These dense shelf water masses are associated with the Ice Shelf Waters and are the Weddell Sea counterparts of those found in the Ross Sea. Waters with salinities above 34.7 and temperatures near freezing constitute Western Shelf Water (WSW), which is analogous to HSSW in the Ross Sea (Table II). This water mass is formed by brine rejection during sea ice freezing on the shallow shelf in the southern Weddell Sea (Mosby, 1934; Foster, 1972) and is the densest water mass on the shelf. LSSW is also present in the Weddell Sea, as is Eastern Shelf Water (ESW), which has salinities of 34.3–34.4 and temperatures near freezing (Table II) (Carmack, 1977). Other water masses present in the western

Weddell Sea are AASW, Winter Water and Ice Shelf Water. The latter water mass is found beneath the floating ice shelves in the Weddell Sea and is probably formed from mixing of WSW and meltwater (Carmack and Foster, 1975; Nicholls and Jenkins, 1993).

The warmer CDW is not present on the western Weddell Sea continental shelf at depths shallower than 750 m. However, in the Weddell Sea, a water mass termed Weddell Deep Water (WDW; e.g., Gordon et al., 1984), which is analogous to CDW, mixes with Winter Water to produce Modified Weddell Deep Water (MWDW), which is found over most of the continental shelf (Foster and Carmack, 1976; Foldvik et al., 1985a). This water has temperatures between −1.5 and −0.5°C and salinities of 34.45–34.65. The *T–S* properties in the eastern Weddell Sea (Fig. 35.5*D*) are similar to those in the western Weddell Sea, except for the more prominent presence of mWDW. The dense Ice Shelf Waters are clearly present, as is AASW.

In the Caird Coast subregion (Fig. 35.5*E*), WSW, MWDW, HSSW and LSSW are present; however, the dense shelf waters are not as pronounced as in the southwestern Weddell Sea. Once again, CDW and AASW are prominent water masses. Farther eastward along the Princess Martha Coast (Fig. 35.5*F*), the water mass structure has returned to one consisting primarily of CDW and AASW. The cold, saline water masses observed in the Weddell Sea are not present.

4.3. *General T–O_2 Properties*

Dissolved oxygen is an additional measurement that can be used to characterize water masses overlying the Antarctic continental shelf. The T–O_2 diagrams constructed for the five large regions (Fig. 35.6) have generally the same basic structure. At one extreme is an oxygen minimum (4–4.5 mL L^{-1}) associated with warm (>0°C) water, which is characteristic of CDW. At the other extreme is high oxygen (6–7 mL L^{-1}) associated with near-freezing temperatures, which is characteristic of Winter Water (Sievers, 1982; Carmack, 1990). Oxygen values in excess of 7.5 mL L^{-1} are associated with AASW (Carmack, 1990).

Variations to the basic T–O_2 structure occur in the Ross and Weddell Seas (Fig. 35.6*A*,*E*), where oxygen values of 6.5–7.5 mL L^{-1} are associated with temperatures at or below the freezing point. These well-oxygenated waters are associated with the HSSW and Ice Shelf Waters that are formed on the continental shelf in these regions (Carmack, 1990).

4.4. *Horizontal Temperature Distributions*

Horizontal temperature distributions at specific depths provide insight into the potential transport pathways followed by various water masses. Thus horizontal temperature distributions at 300 m were constructed for the Ross Sea, the Antarctic Peninsula and Bransfield Strait, and the Weddell Sea regions. The data distribution in the other regions was not sufficient to construct horizontal distributions.

Ross Sea

The temperature distribution at 300 m constructed from the NODC data set for the Ross Sea (Fig. 35.7*A*) shows that the water over the continental shelf is mostly colder than −0.5°C. Temperatures decrease onshore to values of almost −2°C, with the coldest water found in the western Ross Sea along the coast of Victoria Land.

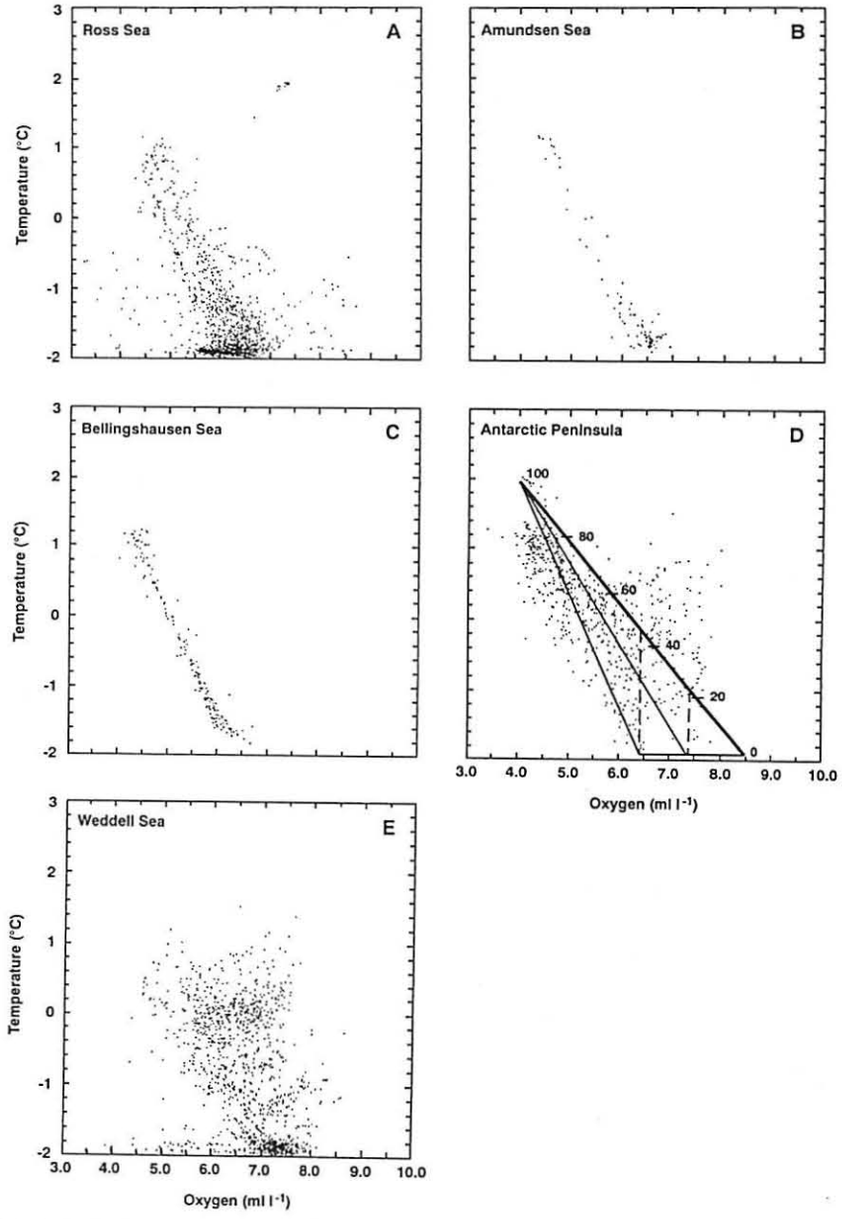

Fig. 35.6. In situ temperature–oxygen diagrams constructed from the NODC hydrographic data set for the (*A*) Ross Sea, (*B*) Amundsen Sea, (*C*) Bellingshausen Sea, (*D*) Antarctic Peninsula and (*E*) Weddell Sea. The heavy line shown in panel (*D*) connects undersaturated (4.0 mL L^{-1}) warm (2°C) CDW with fully saturated surface water (8.54 mL L^{-1}) at the freezing point (−1.86°C). The thinner lines connect CDW with the range of oxygen values observed for Winter Water (6.5–7.5 mL L^{-1}). The dashed vertical lines represent the required proportions of CDW and fully saturated water that are needed to produce the observed Winter Water oxygen values.

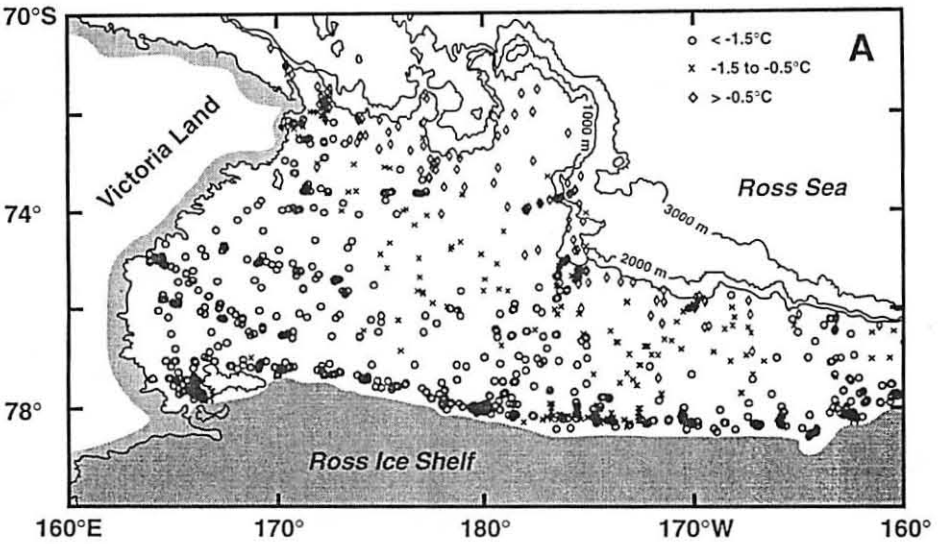

Fig. 35.7. (*A*) Horizontal temperature distribution at 300 m constructed from the NODC hydrographic data set for the Ross Sea. The temperature range corresponding to the different symbols is shown. (*B*) Horizontal temperature distribution at 300 m constructed from CTD and XBT observations made in and around Bransfield Strait. Small dots indicate the distribution of the stations used to construct the temperature distribution. (Adapted from Capella et al., 1992b.) (*C*) Horizontal distribution of Modified Weddell Deep Water (MWDW) constructed from observations from several cruises made in the southwestern Weddell Sea. (Adapted from Foldvik et al., 1985a.)

Water warmer than −0.5°C is found along the outer shelf slope region, and the onshore–offshore pattern of this water tends to follow the outer shelf isobaths. Onshelf movement of water warmer than −0.5°C is associated with across-shelf depressions in bathymetry, and at 300 m the penetration of this water is limited, which is consistent with the patterns seen in across-shelf vertical temperature sections from the Ross Sea (Jacobs et al., 1985). As a comparison, Locarnini (1994) shows that the potential temperature on the σ_0 surface corresponding to 27.78 kg m^{-3} (depths of 100–400 m) is below −1.0°C in the eastern Ross Sea, along the Ross Ice Shelf and close to the coast in the wesern Ross Sea. However, the temperature distribution from Locarnini (1994) shows water warmer than 0°C on the continental shelf near 175°E and 75°S. The Ross Sea composite temperature distribution (Fig. 35.7*A*) does show a region of warmer temperatures, up to −0.5°C, extending across the shelf at this location, but water warmer than 0°C is not indicated. Locarnini (1994) attributes this warmer water to the influence of LCDW.

Antarctic Peninsula–Bransfield Strait

Capella et al. (1992b) present an analysis of the horizontal temperature distribution at 300 m in Bransfield Strait that is based on XBT and limited CTD measurements. At this depth the primary feature in the horizontal temperature distribution (Fig. 35.7*B*) is the warmer water associated with CDW. Water with temperatures characteristic of CDW (>1°C) enter Bransfield Strait through the gap between Smith and Snow

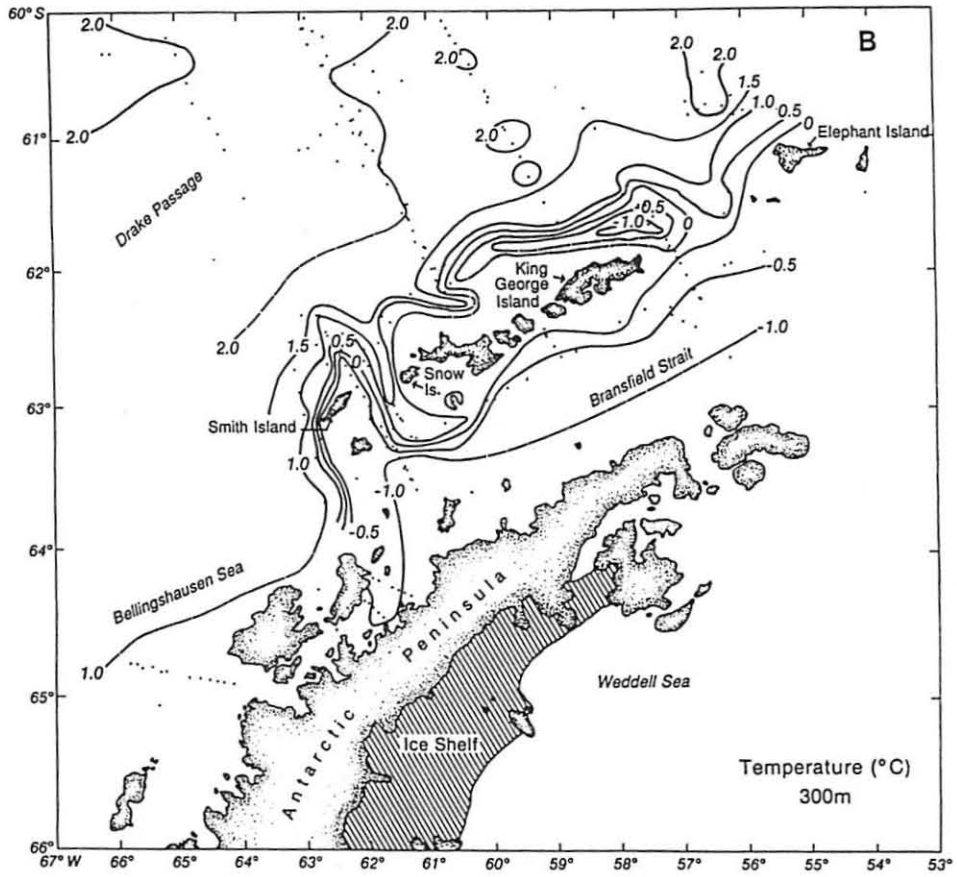

Fig. 35.7. (*Continued*)

Islands. A similar intrusion of CDW was seen in hydrographic measurements made during the First International BIOMASS Experiment (FIBEX; Sievers, 1982; Stein, 1983; Stein and Rakusa-Suszczewski, 1983) and in the western Bransfield Strait as part of the Research on Antarctic Coastal Ecosystem Rates (RACER) field programs (Niiler et al., 1991). The 300-m temperature distribution (Fig. 35.7*B*) shows CDW extending along the southern flank of the South Shetland Islands and as far east as Elephant Island. A temperature boundary separates CDW from the colder waters of Bransfield Strait (Capella et al., 1992b; Stein and Heywood, 1994). Limited penetration of CDW from Drake Passage into Bransfield Strait and spreading along the southern flank of the south Shetland Islands are consistent with the patterns obtained from a *T–S* analysis for this region (Hofmann et al., 1996). The cold (<0°C) water seen at 300 m to the north of the South Shetland Islands is associated with the Polar Slope Current (Nowlin and Zenk, 1988). This current is narrow (10 km) and is found at depths of 400–600 m in this region (Hofmann et al., 1993).

Temperature measurements west of the Peninsula were limited, but 1°C, which is indicative of mCDW, occurs on the continental shelf west of Bransfield Strait (Fig.

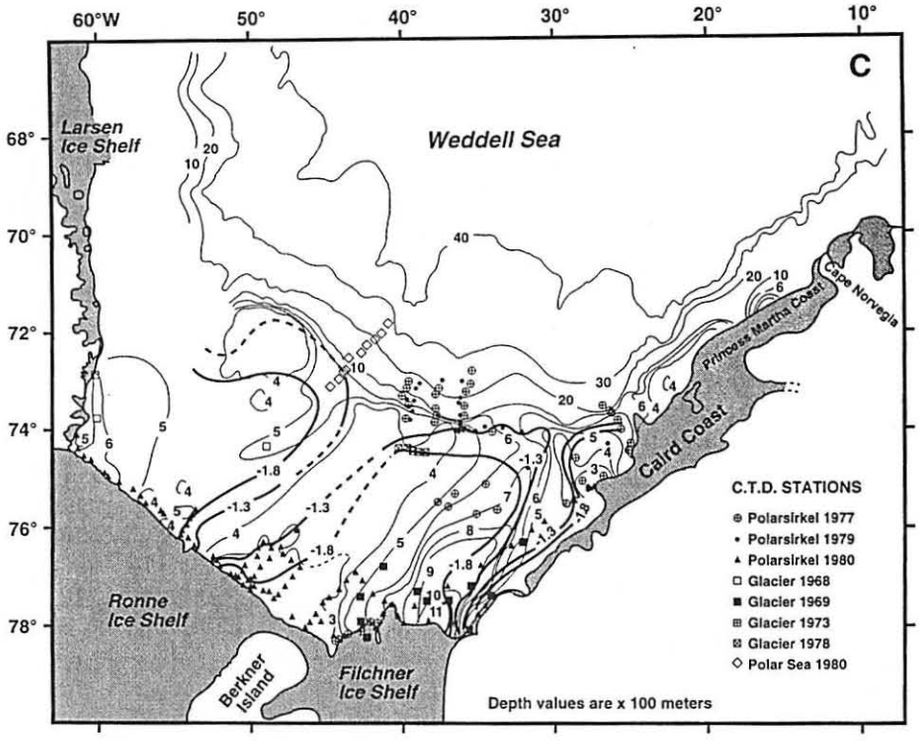

Fig. 35.7. (*Continued*)

35.7*B*). Recent studies indicate that mCDW floods this shelf below 200 m, extends onshore to the inner shelf area and is present in all seasons (Klinck et al., 1994; Smith et al., 1995, Hofmann et al., 1996; Smith et al., in press).

Western Weddell Sea

The distribution of mWDW, which corresponds to the deep temperature maximum, in the southwestern Weddell Sea is shown in Fig. 35.7*C*. The −1.8°C isotherm indicates the maximum extent of this water mass, while the −1.3°C isotherm represents the core of this water on the shelf. This water mass is formed by mixing of WDW and Winter Water at the shelf break and then moves across the shelf at preferred locations (Foster and Carmack, 1976; Foldvik et al., 1985a). MWDW is typically found between 300 and 400 m and forms the deep part of the westward-flowing coastal current (Foldvik et al., 1985a), which is described below. The horizontal temperature distribution indicates that MWDW is found on the inner shelf along the Caird Coast. This water mass is then deflected offshore at about 30°E at the Filchner Depression. To the west of the Filchner Depression, this water mass again extends across the shelf. Thus the distribution of this water mass on the continental shelf in the southwestern Weddell Sea appears to be controlled by bathymetry. As in the Ross Sea, water warmer than −1.0°C is not found on the continental shelf at this depth.

5. Circulation

5.1. Tidal Circulation

Observations of water elevation around the Antarctic are relatively rare due to the small number of permanent land-based research stations and the difficulty of making measurements in ice. Until 1980, almost half of the elevation observations were along the Antarctic Peninsula, and a quarter of the remaining observations were from the Ross Sea (Lutjeharms et al., 1985). Essentially no tidal measurements have been made on the coast between the Bellingshausen Sea and the eastern edge of the Ross Sea.

Analysis of the available tidal measurements from the Ross Sea show the diurnal constituents (O_1 and K_1) to be dominant, with a distinct fortnightly modulation (Pillsbury and Jacobs, 1985; Dunbar and Leventer, 1991; Nittrouer et al., 1992). Moreover, the amplitude of the diurnal tides is large due to a near resonance in this region. Analysis of tidal measurements from the Antarctic Peninsula shows the tides to be mixed with slight diurnal dominance (Amos, 1993; Klinck, 1995). Measurements of tides in the Weddell Sea are mainly from gauges deployed at the South Orkney Islands, although there are a few short records from instruments deployed at the edge of the ice shelves in the south. These records indicate that the tides can be either diurnal or semidiurnal, depending on location (Lutjeharms et al., 1985; Foldvik et al., 1985b).

In lieu of direct observations for the entire region between 150°E and the Greenwich Meridian, the solution from a global tidal model (Egbert et al., 1994), which is based on satellite altimetric observations, was used to estimate the strength of the tidal variations over the Antarctic continental shelf. Of the eight tidal constituents included in the model, only two semidiurnal components (M_2 and S_2) and two diurnal (K_1 and O_1) have a corange above 0.1 m (Fig. 35.8). The tides over continental shelf between 150°E and 60°W are mixed but are dominated by the diurnal constituents (Fig. 35.8*C*,*D*). In the Weddell Sea, however, the tides are mixed but dominated by the semidiurnal components (Fig. 35.8*A*,*B*). These trends agree with the small number of available observations.

The corange for the M_2 constituent is small (less than 0.1 m) throughout the Pacific sector but increases to 0.2 m just west of the Ross Sea (Oates Coast) and at the northeastern tip of the Antarctic Peninsula (Fig. 35.8*A*). On the northwestern edge of the Weddell Sea, the corange increases to 0.7 m, is above 0.5 m throughout the central Weddell Sea and maintains values above 0.4 m along the coast as far east as the Greenwich Meridian. The corange for the S_2 constituent follows the same general pattern but with smaller values (Fig. 35.8*B*).

The coranges for the diurnal components are generally largest at the Antarctic Coast and decrease toward the north. The K_1 constituent has corange isolines that are largely zonal, with the entire coast being above 0.3 m (Fig. 35.8*C*). Values as high as 0.4 m occur in the western Ross Sea and the southwestern Weddell Sea. The corange for the O_1 constituent is above 0.2 m along the coast, with the Ross and Weddell Seas again having the largest values (Fig. 35.8*D*).

The flow speed for the different tide constituents can be calculated from the global tidal solution. The peak flow speed for the semidiurnal constituents is generally less than 0.01 m s^{-1}. However, maximum speeds of 0.05 and 0.03 m s^{-1} for the M_2 and S_2 constituents, respectively, occur at the northern tip of the Antarctic Peninsula. The diurnal constituents are everywhere greater than 0.01 m s^{-1} and increase to 0.02 m

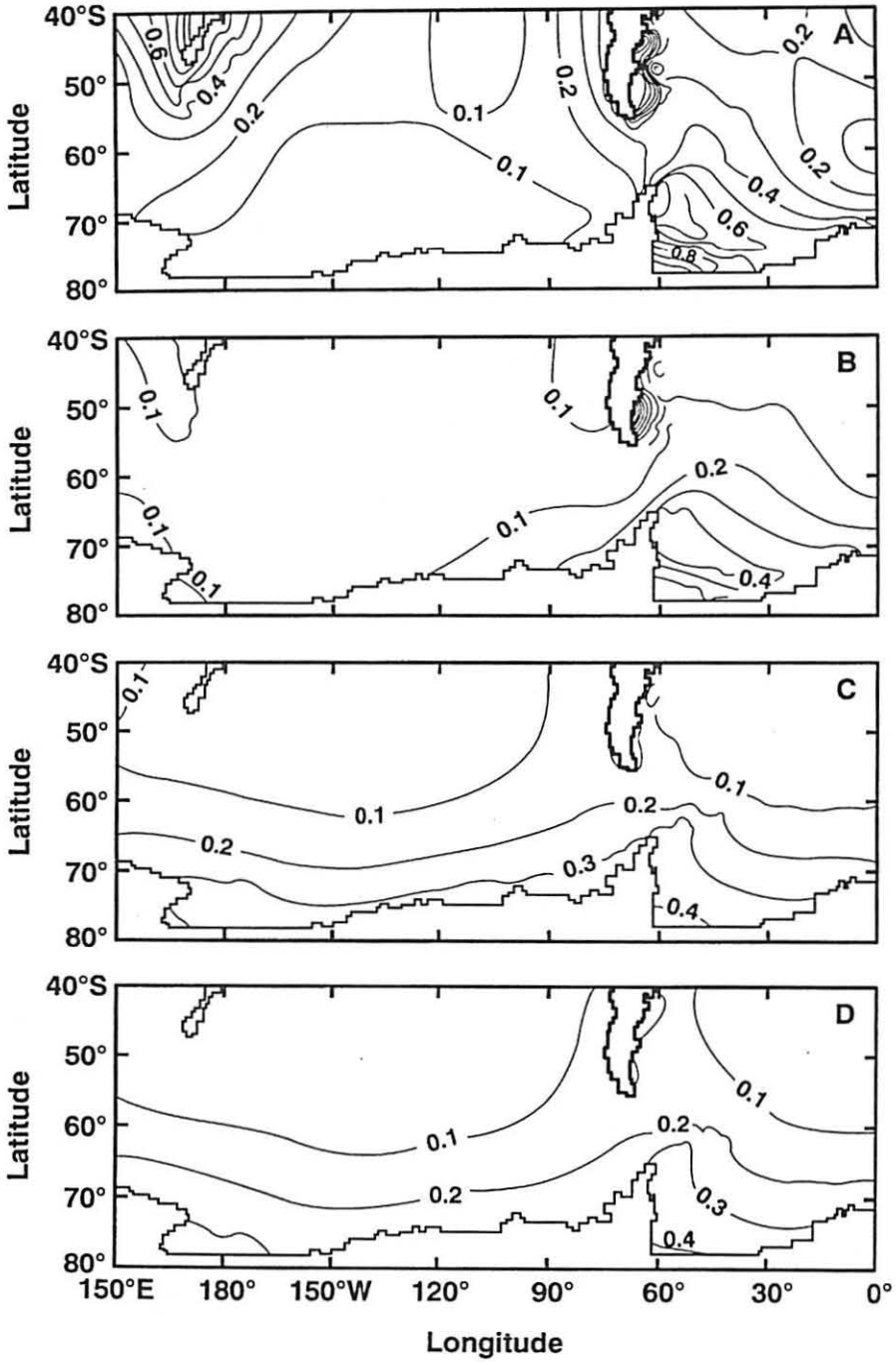

Fig. 35.8. Amplitude (m) of surface tides for the (*A*) M_2, (*B*) S_2, (*C*) K_1 and (*D*) O_1 tidal constituents obtained from the global tidal model given in Egbert et al. (1994).

s^{-1} along the coast. The highest speeds (0.04 m s^{-1}) for the K_1 constituent occur near the South Shetland Islands.

5.2. *Regional Circulation*

A description of the circulation over the Antarctic continental shelf between 150°E and the Greenwich Meridian does not exist; however, descriptions of the circulation in a few smaller subregions are available. Much of what is known about the circulation over the Antarctic continental shelf is based on hydrographic observations. Some surface drifter observations are available for the Antarctic Peninsula region, and limited current meter measurements have been made on the continental shelf in the Ross and Weddell Seas. These are discussed in the following sections.

Ross Sea

Bottom current measurements made in the Ross Sea in January and February 1968 with an instrument deployed from a ship (Jacobs et al., 1970) showed that the flow on the continental slope was generally parallel to topographic contours. Flow on the shelf was to the west or to the north with speeds below 0.1 m s^{-1}.

Moored current meter observations were made at 200- to 500-m depths at about 175°E near the Ross Ice Shelf (Fig. 35.9) from late January to mid-August 1978

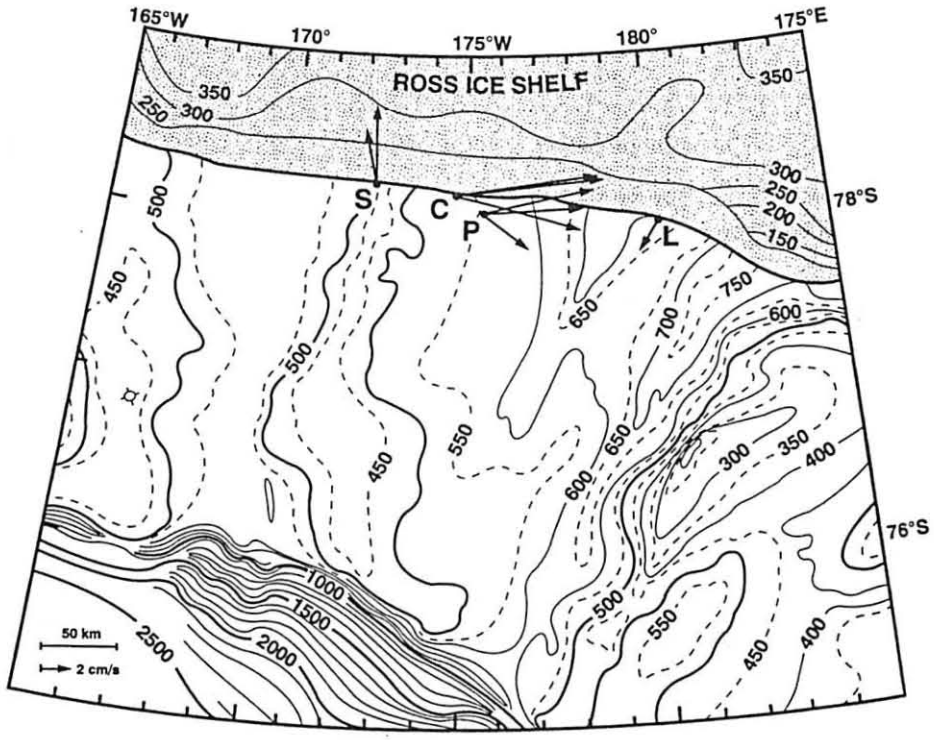

Fig. 35.9. Mean current vectors calculated over 354 days (sites S, C and P) and 204 days (site L) from current meters deployed in the Ross Sea. Ice shelf contours represent ice thickness. Bottom contours are in meters. (Adapted from Pillsbury and Jacobs, 1985.)

and from February 1983 to January 1984 (Pillsbury and Jacobs, 1985). These measurements show that the mean flow was primarily to the west and south with speeds of 0.05–0.09 m s^{-1}. Current velocities averaged higher in the winter, with maximum velocities up to 0.4 m s^{-1}. The multi-instrument moorings showed only a slight decrease in flow with depth.

Kinetic energy spectra calculated from the current meter measurements showed that the lunisolar diurnal (K_1) and principal lunar (M_2) tidal components are the most energetic. Considerable energy was also found at periods between 10 and 100 days. The primary difference noted in the energy spectra was an increase in the winter from May to July, which Pillsbury and Jacobs (1985) attributed to enhanced thermohaline activity. Energy at the inertial period was found to be considerably less than that observed on lower-latitude continental shelves. Ice cover isolates the Ross Sea shelf waters for much of the year and as a result reduces the energy input at this frequency from intense storms.

Analysis of the temperature records from the current meter moorings showed strong seasonal changes from November to April that were attributed to the across-shelf movement of warm water associated with CDW. Pillsbury and Jacobs (1985) suggested that across-shelf movement occurs in summer after sea ice production ceases and the denser shelf waters are not being renewed. At this time the dense waters are eroded from the top by mixing with the warmer, fresher surface water and continue to spill off the shelf at the bottom. The net result is that CDW moves onshore at middepths.

Several studies (e.g., Ainley and Jacobs, 1981) have suggested that the circulation in the Ross Sea is composed of a single gyre; however, the differences in the temperature and salinity characteristics in the western and eastern Ross Sea (Fig. 35.4*B*,*C*) would suggest otherwise. Moreover, a recent analysis (Locarnini, 1994) that used long-term current measurements from the Ross Sea (DeMaster et al., 1991; Dunbar and Leventer, 1991) and water mass properties suggests that the circulation in the Ross Sea below the surface mixed layer is composed of two anticyclonic gyres, with the western gyre ending near 176°W and the eastern gyre beginning at about 172°W. In between, the two gyres are connected by the cyclonic flow described by Pillsbury and Jacobs (1985). The existence of the western anticyclonic gyre is suggested in the current meter measurements and particle transport patterns given in Jaeger et al. (1996).

Antarctic Peninsula–Bransfield Strait

The first description of the upper water column circulation in Bransfield Strait came from dynamic topography constructed from hydrographic measurements made during the *Discovery* investigations (Clowes, 1934). The surface dynamic topography indicated that part of the eastward flow associated with the Antarctic Circumpolar Current turns into Bransfield Strait between Snow, Smith and Low Islands (Fig. 35.10). This produces a cyclonic meander north of Smith Island which has subsequently been observed in surface geostrophic velocities computed from hydrographic observations made during FIBEX (Stein and Rabusa-Suszczewski, 1983), the Second International BIOMASS Experiment (SIBEX; Stein, 1986; Heywood and Priddle, 1987; Stein and Heywood, 1994) and RACER (Amos et al., 1990; Niiler et al., 1991). The mean maximum surface geostrophic velocity associated with the meander was estimated to be 0.08 m s^{-1} (Niiler et al., 1991). Inside the strait, dynamic topography (Clowes,

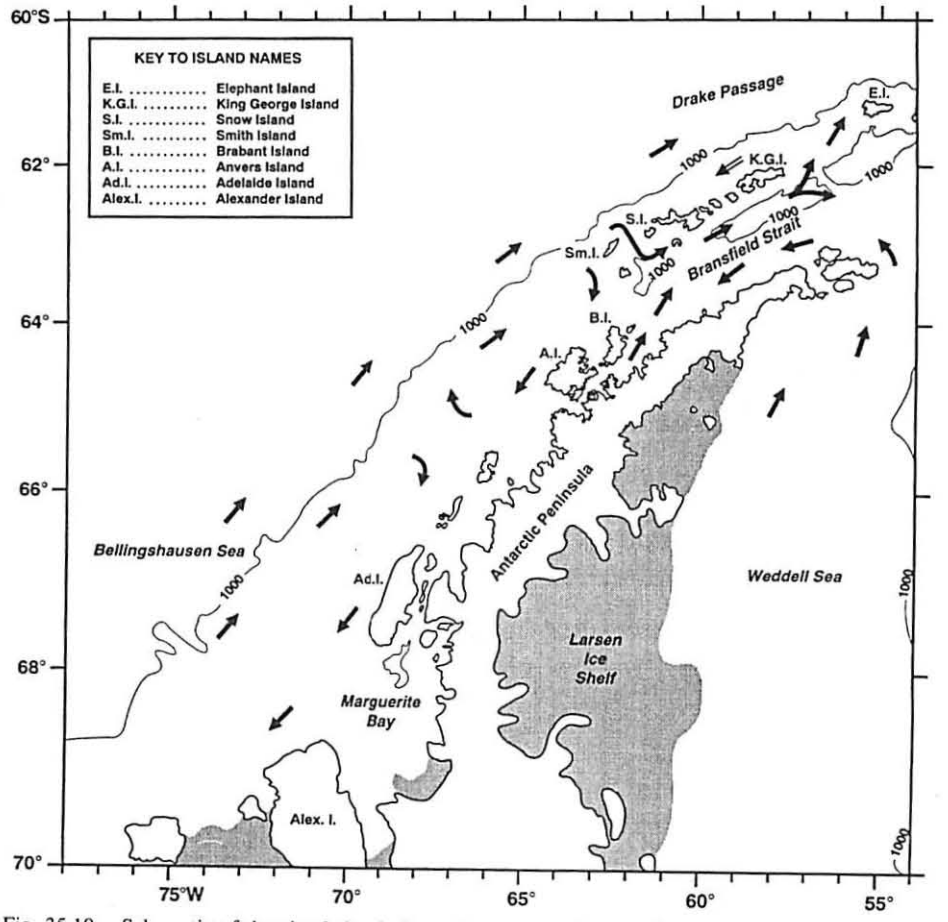

Fig. 35.10. Schematic of the circulation in Bransfield Strait and west of the Antarctic Peninsula constructed from historical data sources. The open arrow to the north of the South Shetland Islands represents the westward-flowing Polar Slope Current. (Adapted from Hofmann et al., 1992b, 1996.)

1934; Stein and Rakusa-Suszczewski, 1983; Stein, 1988) shows that this flow continues eastward along the southern side of the South Shetland Islands. At the eastern end of Bransfield Strait, a branch of the flow leaves the strait between King George and Elephant Islands; the remainder continues eastward.

Drifters deployed during the FGGE show flow into Bransfield Strait from Drake Passage and a surface cyclonic flow within the strait (Hofmann et al., 1996). Average surface velocities in Bransfield Strait computed from the drifter are 0.32 m s^{-1}. Drifters deployed in Gerlache Strait as part of the RACER field programs indicate surface flow to the northeast which persists as a coherent feature into the southwestern Bransfield Strait (Niiler et al., 1990). Once inside the strait, this flow turns to the northeast (Niiler et al., 1991). Surface geostrophic velocities associated with this flow can be in excess of 0.50 m s^{-1} and provide a mechanism for transporting water from the west peninsula shelf into Bransfield Strait.

There are fewer measurements that can be used to describe the circulation west

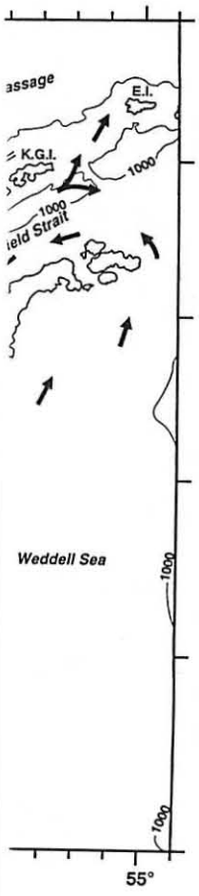

arctic Peninsula con-
nd Islands represents
1996.)

it this flow con-
s. At the eastern
en King George

trait from Drake
l., 1996). Aver-
are 0.32 m s^{-1}.
ograms indicate
the southwest-
is flow turns to
ciated with this
nsporting water

circulation west

of the Antarctic Peninsula than for the Bransfield Stait. Hydrographic observations made in this region as part of the BIOMASS program indicate southward flow along the inner shelf (Kock and Stein, 1978; Stein, 1981, 1982, 1986, 1988). More recently, Stein (1992) presented dynamic topography maps that were constructed from a large-scale hydrographic survey made as part of SIBEX. These show an upper water column circulation that is composed of two cyclonic gyres: one near Anvers and Brabant Islands and one near Adelaide Island. The trajectory followed by a FGGE drifter suggests a cyclonic gyre near Anvers Island (Hofmann et al., 1996). Surface drifters deployed north of Anvers Island as part of the RACER field studies (Niiler et al., 1990) follow a meandering surface circulation in the midshelf region.

The major circulation features described for Bransfield Strait and the west Antarctic Peninsula region were used to construct a schematic of the flow for this region (Fig. 35.10). This circulation shows flow into Bransfield Strait from west of the Antarctic Peninsula, the Weddell Sea and through the gaps between the South Shetland Islands. The latter pathway provides a source of CDW to the northern Bransfield Strait. Thus Bransfield Strait receives a variety of water types which contribute to the complex upper water column structure (cf. Fig. 35.5*B*) that has been described for this region (Stein, 1983, 1986, 1989; Sein and Rakusa-Suszczewski, 1984). Flow out of the strait may also occur along the same pathways as well as at the eastern end. North of the South Shetland Islands, the Polar Slope Current carries water of Weddell Sea origin to the west (Nowlin and Zenk, 1988). Average velocities associated with the Polar Slope Current, as determined from current meter observations, are about 0.10 m s^{-1} (Nowlin and Zenk, 1988). Quetin and Ross (1984) suggested that the westward-flowing Polar Slope Current was the mechanism by which krill embryos released north of the South Shetland Islands were transported to the west, where they were then transported into Bransfield Strait.

Over the continental shelf west of the peninsula, the general circulation is cyclonic. The outer portion of this circulation is provided by the northeasterly-flowing ACC. The inner portion is provided by the southward coastal flow. Within this cyclonic flow, there may be one or more mesoscale gyres.

Western Weddell Sea

On the basis of temperature and salinity distributions, Gill (1973) inferred the horizontal circulation over the continental shelf and slope regions in the Weddell Sea. A main feature of the circulation is the Antarctic Coastal Current, first described by Deacon (1937), which enters the Weddell Sea from the east. This current flows westward with velocities of 0.1–0.3 m s^{-1} and is identified in hydrographic sections by its cold (−1.5°C) and fresh (salinity 34.3–34.4) characteristics. At 27 to 30°E, the current turns offshore and flows along the shelf break. At this time, the Antarctic Coastal Current is identified by a V-shaped region in which the offshore side of the current is separated from the warmer, saltier water by a strong pycnocline, and the onshore side is separated from the colder, saline shelf water. The particular structure is striking because water on either side of the current is saltier than that in the current. This current can be tracked at the shelf break in hydrographic sections to at least 50°W.

Current meter moorings deployed near the shelf break in the southwestern Weddell Sea (Fig. 35.11) in 1968–1969 and 1977–1978 provide two year-long records of the flow (Foldvik et al., 1985b). The mean current direction is primarily along iso-

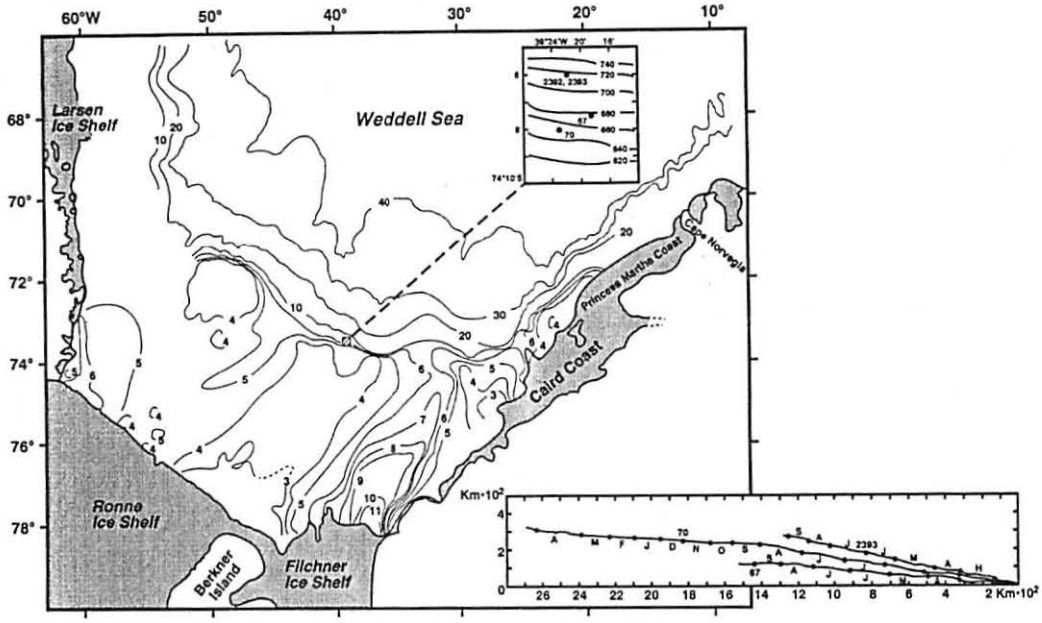

Fig. 35.11. Location of current meter moorings deployed in the Weddell Sea in 1968–1969 and 1977–1978. Inset shows the progressive vector diagram obtained from the current meters. Solid circles indicate the beginning of each month, and months are indicated by the letters. The axes are relative to magnetic west and north. Instruments 67 and 70 were deployed in February 1968; instrument 2393 was deployed in February 1977. (Adapted from Foldvik et al., 1985b.)

baths to the west (Fig. 35.11), with a small northward component. This flow direction was stable over the time of the current meter records. Mean current velocities were 0.06–0.07 m s^{-1}; however, variations in monthly mean current speed were large, with the average during winter months being almost twice the summer values. The flow direction inferred from hydrography is consistent with that from direct current measurements.

Spectral analysis of these current meter records indicated that the across-isobath component of the flow had the most energy between 1.5 and 3 days. The along-isobath flow component exhibited the most energy at periods longer than 2.5 days. However, the energy fluctuations had a strong seasonal component, with little energy in the low-frequency band in the winter when the ice cover reaches is maximum extent. Foldvik et al. (1985b) suggest that the reduction of energy in late winter may result from low-pressure systems passing farther north in the winter than in the summer, reduced input of wind energy to the ocean due to the ice cover, or a reduction in static stability in the winter. Middleton et al. (1982) also analyzed low-frequency motions in the southwestern Weddell Sea from current meters deployed between January 1977 and January 1980. Energy in long-period motions over the continental slope is due mainly to baroclinic effects, and barotropic motions dominate over the shelf. Further, motions on time scales longer than five days are due primarily to wind effects, while motions with scales of two to five days are due to continental shelf waves.

6. Theoretical Circulation Studies

Theoretical studies of circulation on the Antarctic continental shelf consider a number of processes and achieve different levels of realism. In this section we discuss process-based models, large-scale circulation models that include the Antarctic continental shelf, and regional circulation models that have been constructed for specific regions of the Antarctic continental shelf system.

6.1. Process Models

Process models developed for Antarctic shelf continental shelf systems consider the force balances that drive the circulation and thermodynamic processes that create the various water masses that are observed on the continental shelf, the forces that drive circulation under permanent ice shelves, and the dynamical processes associated with latent and sensible heat polynyas. Even though some of these modeling studies are specific to certain ice shelves or polynyas, they are included in the discussion of process-based models given below.

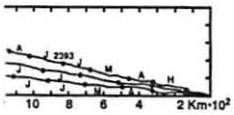

in 1968–1969 and
meters. Solid circles
axes are relative to
nstrument 2393 was

is flow direction
velocities were
eed were large,
ner values. The
n direct current

across-isobath
ays. The along-
than 2.5 days.
ith little energy
es is maximum
in late winter
winter than in
ice cover, or a
analyzed low-
eters deployed
otions over the
motions dom-
e days are due
lays are due to

Circulation and Water Mass Formation

Gill (1973) provided a comprehensive discussion of the processes underlying circulation and thermodynamics of dense water formation on the Antarctic continental shelf. The study was focused on the Weddell Sea, but the analysis also applies to the Ross Sea, where dense water formation occurs. On the basis of dynamical arguments, Gill (1973) showed that the double salinity front, the V-shaped front, at the shelf break is formed from cold, fresh water that is produced by melting of surface ice and downwelling forced by the easterly winds. In effect, a downwelling jet brings in fresh water from farther east.

Gill (1973) also used mixing models to consider the processes underlying the formation of Weddell Bottom Water at the shelf break. Dense, salty water is formed on the shelf as a result of brine rejection due to ice formation; however, considerable freezing is required to produce the amount of salt needed for water formation. Gill (1973) proposed that offshore winds near the coast transport pack ice offshore, thereby exposing more water to heat loss and freezing. Once formed, the dense shelf water must flow off the shelf if bottom water production is to be a continuous process. For the deep water to flow offshore geostrophically, there must be an alongshore tilt of the density surfaces such that the water becomes denser to the west. This alongshore density structure is observed in the southern Weddell Sea and also in the Ross Sea. Gill (1973) proposed that Weddell Bottom Water production is the result of the mixing of HSSW and offshore CDW. This mixing occurs at the base of the V-shaped salinity front at the shelf break.

An analytical model of buoyancy-forced flow on the Antarctic continental shelf was developed by Killworth (1973). The model included sloping bottom topography, wind and surface buoyancy flux, but did not account for nonlinearities in the equation of state for seawater. Also, the model dynamics were constrained to be two-dimensional (vertical plane) and geostrophic, with turbulent boundary layers. The net buoyancy flux over the entire model was balanced with positive buoyancy flux (cooling) in the south and negative (warming) in the north. These dynamical choices and fluxes produce a circulation that is confined primarily to frictional boundary layers and a weak interior circulation. With only buoyancy forcing, no matter how strong,

bottom water was not created; wind forcing was required to produce an overturning circulation.

A two-layer model of the horizontal, baroclinic circulation on the Antarctic continental shelf (Killworth, 1974) considered the dynamics of flow of dense water off the shelf. This model included a flat bottom and a vertical structure in which both model layers were of equivalent thickness. Vertical mixing across the pycnocline was included to mimic thermodynamic effects. Both asymptotic and numerical solutions were obtained for the governing equations.

The surface forcing applied to the model was invariant alongshore, but along-shelf variaion in the pycnocline elevation was required to drive a geostrophically balanced offshelf flow in the lower layer. This alongshore gradient occurs in the model due to coastal boundaries (representing the meridional boundaries at the western end of the Ross and Weddell Seas). The numerical model solution indicated buoyancy-forced surface flow to the south and east, with bottom flow north and westward. The densest water occurred along the western boundary, which is in agreement with observations. Seasonally varying surface buoyancy flux produced no seasonal variation in the exchange of dense water after initial transients decayed.

Ice Shelf

Unique to the Antarctic continental shelf are the thick permanent ice shelves. These shelves are important because they drive a circulation that draws in warm, salty water at depth and expels cold and fresher water (Ice Shelf Water) near the surface (Nøst and Foldvik, 1994; Hellmer and Jacobs, 1995). This circulation is driven by buoyancy changes in the water due to the decrease in the freezing point of water with depth. The warmer shelf water is drawn in and under the ice shelf at a depth below 500 m, where it is strongly cooled by melting ice from the bottom of the shelf. The water becomes fresher and hence lighter, so it flows upward. There is some refreezing of the water as it moves upward; however, the inflow of warm shelf water is the heat source that keeps the circulation running.

An analytical model of this circulation constructed for the Filchner–Ronne Ice Shelf in the Weddell Sea (Nøst and Foldvik, 1994) determined that the critical factor in the circulation was the temperature and salinity of the source water, not the details of entrainment or melting under the ice. The situation in the southern Weddell Sea allows several possible circulation paths; however, Nøst and Foldvik (1994) conclude that WSW flows eastward from the Ronne Depression into the Filchner Depression, where the densest water is created. This dense water is proposed as a critical component of Weddell Sea Bottom Water. This model was also applied using conditions from the Ross Sea to show that Ice Shelf Water is formed from LSSW.

A second study of the southern Weddell Sea (Jenkins and Doake, 1991) deduced from observations under Ronne Ice Shelf that HSSW (or WSW) is drawn in as narrow currents along the edges of the deep areas. Outflow of Ice Shelf Water is largely along the western boundaries, along the continent and along Berkner Island.

Potter and Paren (1985) constructed a simple model for flow under the ice shelf in George VI Sound, which is south of Marguerite Bay along the western side of the Antarctic Peninsula. Observations of water characteristics and flow made at a number of places along the sound were used with the model. Results show that CDW flows under the ice southward at depth and colder, fresher water flows out (north) in the

upper 200 m, with the strongest flow on the western side of the sound. The outflowing water is about −1.7°C and 33.6.

Hellmer and Jacobs (1995) used year-long time series of temperature and salinity from two locations off the Ross Ice Shelf to force a vertical plane model of Ice Shelf Water production. There is a seasonal variation water characteristic at the outflow, and the model generally captured the proper variations. The timing of peak outflow in November and December is not quite correct, but the magnitude and duration are in agreement.

Coastal Polynyas

Several models have been developed to estimate the size and duration of coastal polynyas and the resulting heat and salt flux. The first quantitative calculation is due to Pease (1987), who made the assumption that a polynya achieves a stable size when the production rate of sea ice over open water matches the rate at which ice is transported to the retreating ice edge (e.g., a latent heat polynya). These processes are controlled by the atmospheric temperature and wind speed. The size of polynyas is strongly affected by air temperature, which changes the seawater freezing rate. The effect of wind is weak at speeds greater than 5 m s^{-1} because the wind affects both the freezing rate and the export rate. The maximum size of a polynya is shown to be VH/F, where V is the speed of retreat of the offshore ice shelf, H the collection depth for frazil ice, and F the frazil ice production rate. The time scale to reach a stable size is $3.0H/F$, which is relatively short for the cases discussed (0.5–4 days). The results of this model compare well to observations from two polynyas in the Bering Sea.

A time-dependent model of latent heat polynyas (Ou, 1988) is an extension of the Pease (1987) model that allows for finite drift speed of the frazil ice, which is estimated from the wind speed. This model results in faster opening of polynyas because the retreating sea ice edge does not accumulate as much as frazil ice, due to its finite transport speed. Short-time-period variations of the atmospheric forcing are shown to be unimportant because of the finite time required for the polynyas to adjust to new conditions.

A second extension to the Pease (1987) model considers the velocity of the offshore sea ice edge as well as of the frazil ice and the relationship of these vectors to the coastline orientation (Darby et al., 1995). The relative directions are shown to have important effects on the steady-state size and the development time of the latent heat coastal polynyas. The model also shows that polynyas do not react to coastline geometry with small scales. Comparison of the model with the Terra Nova Bay and the St. Lawrence Island polynyas show the validity of the model.

The influence of polynyas on the salinity of the underlying water is considered by Grumbine (1991). Polynyas in the model are controlled by wind stress curl and salinity flux due to seawater freezing. The ocean model has two levels in the vertical, ignores time derivatives in the governing equations and holds the barotropic circulation constant. Twenty simulations are considered and each simulation lasts 32 years. This study reveals that polynyas are critical in the formation of high-density water on the continental shelf and that the formation of polynyas depends both on Ekman divergence and the seawater freezing rate.

6.2. *Large-Scale Circulation Models*

Several global ocean modeling studies have been undertaken, most of which are based on grids with resolutions that are larger than 2° of latitude and longitude. As a result, the simulated circulation poorly resolves the coastal flow around Antarctica. However, two recent circulation models consider spatial scales on the order of a few tens of kilometers: a global model (Semtner and Chervin, 1988, 1992) and a Southern Ocean model, the Fine Resolution Antarctic Model (FRAM: FRAM Group, 1991; Webb et al., 1991). Both models use ocean depths that are extracted from a 5′ bathymetry and smoothed over a spatial scale of about 1° of latitude and longitude. The effect of this smoothing is to greatly reduce the area of the continental shelf such that it is represented only by general features. Also, atmospheric forcing in coastal areas is very important, but little effort was expended to incorporate realistic forcing in these regions in the global circulation and FRAM calculations. The focus of these modeling studies was on realistic simulation of large-scale ocean circulation; therefore, the lack of emphasis on realistic flows over continental shelf regions is not surprising.

The simulated vertical temperature and flow obtained from the six-year average solution of the FRAM calculation for the Antarctic Peninsula continental shelf region are given in Hofmann et al. (1996). CDW is evident away from the coast in the vertical temperature distribution. However, the bathymetry used for this calculation included a much reduced continental shelf; thus penetration of CDW onto the continental shelf west of the Antarctic Peninsula is not observed. The simulated circulation shows primarily weak alongshore flow to the northeast. There is no indication of gyres on the shelf or a southwestward current near the coast. This lack of agreement with observations is probably due in large part to the crude representation used for the shelf bathymetry and, possibly, improper specification of wind and buoyancy forcing.

6.3. *Regional Circulation Models*

Antarctic Peninsula–Bransfield Strait

The time-dependent, three-dimensional, primitive equation model developed by Semtner (1974) was used to simulate the circulation in the region around the Bransfield Strait and South Shetland Islands. The modifications made to this circulation model to adapt it for this region are described in Capella (1989), and some of the simulated circulation patterns are shown in Capella et al. (1992a). A representative simulated surface (0–50 m) circulation from January is shown in Fig. 35.12. West of about 60°W the effect of the Antarctic Peninsula is to force the flow, which is oriented along isobaths, in a general northeasterly direction, where it joins the flow of the Antarctic Circumpolar Current. East of 58°W, the flow north of the South Shetland Islands is to the west. Near Elephant Island, a complex circulation develops, which is probably due to the complex topography in this region. Flow in the southeastern Bransfield Strait is to the west, which is the result of flow from the Weddell Sea into the strait. Surface flow in the northern strait is primarily to the north. The surface flow at the western end of Bransfield Strait is continuous with that farther west. The simulated circulation pattern shown in Fig. 35.12 is primarily the result of the Ekman response to wind forcing. Consequently, the simulated circulation from other months (Capella, 1989) have variations in the upper 150 m that are produced by the seasonal

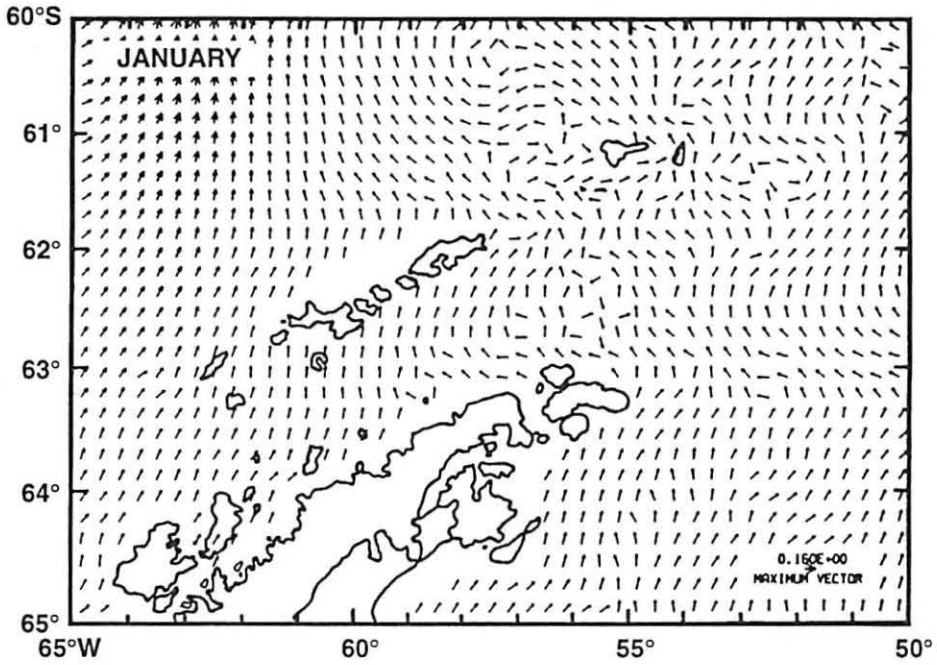

Fig. 35.12. Simulated surface circulation (m s^{-1}) in the Bransfield Strait–Antarctic Peninsula region in January. The magnitude of the velocity is indicated by the size of the arrowhead. The geographic features are identified on Fig. 35.10. (Adapted from Capella et al., 1992a.)

changes in the wind forcing. These are primarily changes in the intensity of the flow; the general surface circulation pattern remains the same. The general features of the simulated flow agree with those seen in the schematic flow constructed from historical observations (cf. Fig. 35.10). However, the details of the simulated flow, such as the occurrence of mesoscale gyres, differ. The model by Capella (1989) did not include sea ice, and to date, no attempts have been made to implement a coupled sea ice–ocean circulation model for the west Antarctic Peninsula region.

Weddell Sea

A model of wind-driven circulation in the Weddell Sea (Gordon et al., 1981) shows that the circulation has the general character of a polar gyre, which is forced by the surface wind stress. Dynamic topography of the surface relative to 500 db is in general agreement with the wind-driven circulation. The eastern end of the Weddell Gyre extends to about 40°E, and the simulated circulation shows a considerable part of the southern limb of the gyre to be over the continental shelf. There is very little dynamic topography away from the coastal boundaryof the gyre.

A coupled sea ice–mixed layer–pycnocline model was developed to investigate ice and upper ocean circulation dynamics in the Weddell Sea (Lemke et al., 1990). This model couples a two-layer dynamic-thermodynamic sea ice model (Hibler, 1979), which includes a prognostic snow layer with a one-dimensional prognostic mixed-layer model (Lemke, 1987). The focus of this study is on the entire Weddell Sea, so the shelf regions are not well represented. It is clear from the results that sea

ice production is largest over the continental shelf along the southern boundary of the Weddell Sea, and that sea ice accumulation is largest in the southwestern corner. Furthermore, the snow layer greatly affects ice thickness (Owens and Lemke, 1990) and the seasonal cycle of ice extent is very sensitive to the ice dynamics (Stössel et al., 1990). This study clearly indicates that sea ice is an important factor in Antarctic shelf circulation; however, the details of which processes are important in different areas remains to be determined with models that include the detail of the Weddell Sea continental shelf as well as other regions.

7. Discussion

7.1. Influence of CDW

Distribution

CDW is an important component in structuring the hydrographic properties of the water overlying the Antarctic continental shelf between 150°E and the Greenwich Meridian (Table II). This water mass is found in central Drake Passage at depths of 1000 m or more (Sievers and Nowlin, 1984). Toward the Antarctic shelf, CDW rises in response to the equatorward Ekman transport of surface waters. Hence at the outer shelf, the core of CDW is found at 400–700 m. The continental shelf surrounding the Antarctic is about two times deeper than midlatitude shelves which results in the outer edge of the shelf being about 500 m at the shelf break. At the edge of the continental shelf, UCDW is found at 150–200 m. The relative shallowness of this water mass, coupled with the deep shelf, results in a water mass structure on the shelf that is similar to the deeper offshore waters. This differs from midlatitude shelf systems, where shelf breaks are shallower and shelf waters are not typically oceanic in character. Also, the greater depth of the Antarctic continental shelf reduces the effect of wind mixing to a smaller portion of the water column than is found on midlatitude shelves. The upper 150–200 m undergoes modifications that result from seasonal changes in wind forcing and heat and salt fluxes. However, the deeper waters are not affected by these processes, which allows the oceanic character of the bottom waters to remain intact.

Once on the shelf, CDW mixes with AASW to form a modified version of CDW. As shown by Smith et al. (in press), the amount of mixing each water type needed to form the modified CDW cannot be estimated by simple two-point mixing theory since one of the end members, AASW, undergoes seasonal modification. The onshelf velocities and horizontal diffusion rates needed to maintain the vertical heat loss from modified CDW to AASW on the west Antarctic Peninsula continental shelf were estimated to be 0.002 and 200 $m^2\ s^{-1}$, respectively (Smith et al., in press). Those for salt were estimated to be 2×10^{-5} and 950 $m^2\ s^{-1}$, respectively. The need for different values of horizontal advection and diffusion rates for heat and salt indicates that simple advective or diffusive balances are not sufficient to explain the onshore movement of CDW and the resulting mixing of this water. Smith et al. (in press) suggest that double-diffusive processes are potentially important in the mixing of CDW and AASW.

As an alternative, Potter and Paren (1985) suggested that ice melting in the inner shelf region drives the across-shelf movement of CDW. Essentially the outflow of the more buoyant surface water produced by ice melt is replaced by onshore transport of

CDW at depth. The upwelled CDW provides the heat source that maintains the ice melting and hence the circulation. The across-shelf velocities associated with this circulation were estimated to be 0.006 m s^{-1} (Potter and Paren, 1985). A similar circulation has been suggested to exist in the Ross Sea (MacAyeal, 1985).

CDW potentially has an effect on biological productivity and distributions. For example, it has been shown that the presence of this water mass is important to the reproductive cycle of Antarctic krill (Hofmann et al., 1992a). Also, the coastal waters of the Antarctic support large populations of Antarctic krill and top predators, such as penguins, seals and whales. Thus upwelling of CDW, which is high in nutrients (Sievers and Nowlin, 1984), could provide predictable regions of enhanced production. Also, upwelling of this warm water may provide predictable regions of open water in winter. Therefore, a careful and thorough mapping of the distribution of CDW is essential for understanding the potential effects of climate change on biological production on Antarctic coastal waters.

CDW Entrainment and Salt and Heat Budgets

Sievers (1982) showed that upwelling north of the South Shetland Islands resulted in the injection of CDW into the upper water column. Entrainment of this low-oxygen water has been suggested as an explanation for the undersaturated oxygen concentrations that are associated with Antarctic surface waters (Gordon et al., 1984; Smith and Tréguer, 1994). The oxygen values associated with Winter Water, which undergoes minimal seasonal modification, range between 6.5 and 7.5 mL L^{-1}. Using these values and the temperature corresponding to the oxygen minimum of CDW in the five regions (Table III), the percent mixing between CDW and Winter Water can be estimated as illustrated on Fig. 35.6*D*. This approach assumes that the Winter Water composition is time invariant.

In all the continental shelf regions, the reduction in oxygen of Winter Water requires mixing of 25 and 55% with the low-oxygen CDW (Table III). For a 100-m-thick upper layer, the oxygen values suggest an annual entrainment of 25 to 50 m of CDW (Table III). The range calculated for CDW entrainment in the five regions is similar, as are the annual entrainment rates (Table III). The estimates in Table III are similar to those obtained for the Weddell Sea (Gordon et al., 1984), Prydz Bay (Smith and Tréguer, 1994) and west of the Antarctic Peninsula (Hofmann et al., 1996). However, the estimated entrainment rates should be used with caution

TABLE III
Summary of the Percent CDW Mixing, Entrainment Rate, Temperature Difference between CDW and Winter Water, and Heat Flux Calculated for the Five Continental Shelf Regions

Region	% CDW	Entrainment Rate (m yr^{-1})	Δ Temperature (°C)	Heat Flux (W m^{-2})
Ross Sea	27–51	26.8–51.1	2.6	10.7
Amundsen Sea	30–54	30.0–53.9	2.7	11.1
Bellingshausen Sea	25–50	24.9–50.1	2.75	11.3
Antarctic Peninsula	24–48	24.0–47.9	3.5	14.4
Weddell Sea	29–51	29.0–51.1	2.25	9.2

since these are derived from limited data in some regions and data that are primarily from the summer. These estimates assume that the summer undersaturation values are typical of the entire mixed layer in winter. The estimates made by Gordon et al. (1984) were based on winter observations only, in which the entire upper 100 m consisted of Winter Water. Moreover, this calculation assumes no contribution from nonconservative processes such as oxidation of organic material and heterotrophic respiration. However, the T–O_2 relationship shown in Fig. 35.6 is distinct, which lends support to the contention that this is the result of conservative processes.

The salt introduced by entrainment of CDW over a year requires an input of fresh water to reduce CDW salinity (34.73) to that of Winter Water (34.00). Assuming a 100-m-thick layer and a range of vertical diffusion coefficients of 10^{-5}–10^{-4} m^2 s^{-1}, a simple salt budget shows that 0.063–0.63 m yr^{-1} of fresh water is needed to produce the Winter Water salinity. Gordon (1981) estimated the assunal maximum freshwater input due to excess of precipitation over evaporation and continental runoff between 60 and 70°S to be 0.40 m yr^{-1}. Estimates for west of the Antarctic Peninsula give annual precipitation rates of 0.45–0.80 m (Domack and Williams, 1990). Annual precipitation rates at Palmer Station on Anvers Island range from 0.40 to 1.00 m yr^{-1}, and those at McMurdo Station in the Ross Sea range from 0.1 to 0.5 m yr^{-1} (e.g., Anon., 1991, 1992, 1993). These precipitation estimates can provide from two-thirds to all of the freshwater needed to balance the salt input. Assuming that the lower rates are more representative, additional fresh water must be supplied from other sources, such as ice melt.

The average rate of heat input by CDW can be estimated by assuming a vertical diffusion coefficient (10^{-4} m^2 s^{-1}) and using the temperature difference between CDW and Winter Water in the five shelf regions (Table III). The heat flux values thus calculated range from 9 to 14 W m^{-2} (Table III), with the Antarctic Peninsula and Weddell Seas having the largest and smallest values, respectively. These values are similar to those estimated for the Weddell Sea (Gordon et al., 1984) and the west Antarctic Peninsula continental shelf (Hofmann et al., 1996). Since the temperature difference between CDW and Winter Water persists throughout the year (Fig. 35.4, 35.5), this estimated heat flux is representative of an annual flux.

The rate at which sea ice can be melted by this range of heat flux is 2.72–4.22 $\times$ 10^{-8} m s^{-1}, which converts to a rate of 0.85–1.3 m yr^{-1}. Potter and Paren (1985) estimated an ice melt rate of 1.1–3.6 m yr^{-1} due to upwelling of CDW west of the Antarctic Peninsula. Pillsbury and Jacobs (1985) estimated that the onshore transport of the CDW in the Ross Sea is sufficient to melt about 150 km^3 yr^{-1} off the base of the Ross Ice Shelf. The salinity budget suggests that a melting rate of 2.06 $\times$ 10^{-8} m s^{-1} (0.63 m yr^{-1}) is needed to provide sufficient fresh water to maintain the salinity associated with Winter Water. Melting of this amount of ice requires about 7 W m^{-2}, which is less than the heat provided by CDW. Thus the heat flux from below is sufficient to melt the required amount of ice, even without the addition of surface heating.

These calculations suggest that the addition of fresh water from ice melt is an important part of the heat and salt budgets of the Antarctic continental shelf. No deep water is formed outside the Ross and Weddell Seas, which are the two regions where modified CDW does not penetrate across the continental shelf at depth (cf. Figs. 35.5*C*,*D*; 35.7*A*,*C*). It may be that the presence of modified CDW near the surface inhibits formation of dense water by preventing ice from forming. Thus some shelf

areas may be regions of ice melt as opposed to a region of ice formation, as has been suggested for the west Antarctic Peninsula shelf (Goerson et al., 1992; Stammerjohn and Smith, 1996).

7.2. *Deep-Water Formation*

A unique and climatologically critical feature of the Antarctic continental shelf is the dense water that is formed in some areas and moves into the deep ocean, creating a worldwide bottom water circulation. This whole-ocean overturning cell has implications far beyond the narrow continental shelf from which it is driven.

Various theories have been advanced for the formation of dense water. However, all generally involve removal of heat by surface cooling and an increase in salinity by freezing. Deep-water production on the Antarctic continental shelf is helped by the presence of salty CDW at the shelf break and a large salt flux that is produced by continued freezing of sea ice, which is moved offshore by winds in the coastal latent heat polynyas.

Since cooling and freezing happen throughout the Antarctic, why is bottom water formation confined to two major regions, the Weddell and Ross Seas? In particular, why is no dense water formed along the coasts of the Amundsen and Bellingshausen Seas, which are at the same latitude as the active water formation regions? Part of the reason may be that the Amundsen and Bellingshausen Seas are at the eastern end of a large embayment, and therefore, following the ideas of Killworth (1974), any dense salty water produced in these regions will be exported to the west to the Ross Sea. Also, the Amundsen and Bellingshausen Seas are ice covered throughout the year (cf. Fig. 35.3), so little sea-ice formation occurs in this area, thus producing a small salt flux. Additionally, the winds may not be sufficient or in the correct direction to transport the new sea ice offshore so that coastal polynyas are opened only infrequently. Finally, this area may be a net import region of ice. Consequently, the summer ice thaw may more than compensate for any winter freezing, giving rise to a net negative buoyancy flux for the area.

Similarly, deep-water formation is not observed along the west Antarctic Peninsula continental shelf. Smith et al. (in press) argue that this arises because the warm modified CDW near the surface over the continental shelf inhibits the formation of sea ice. They also suggest that the atmospheric temperature in this region is not as cold as that over the Weddell and Ross Seas, since this region is not affected by katabatic winds, which are known to be important in deep-water formation in other places around Antarctica (Parish and Bromwich, 1987; Schwerdtfegger and Amaturo, 1979). Thus the west Antarctic Peninsula shelf may be a region of sea ice melt rather than a region of sea ice formation, as suggested by Gloerson et al. (1992).

7.3. *Circulation*

The limited information on circulation in the Ross and Weddell Seas indicate that flow speeds on these continental shelves are similar and that the shelf circulation is composed of one or more gyres. Moreoever, a striking feature in both regions is the strong V-shaped front that occurs at the shelf break (Fig. 35.13). This strong gradient in temperature and salinity over the Antarctic shelf break has been referred to as the Antarctic Slope Front (Ainley and Jacobs, 1981; Jacobs, 1986, 1991). This front may be the result of wind and buoyancy forcing, and it supports a westward flow along

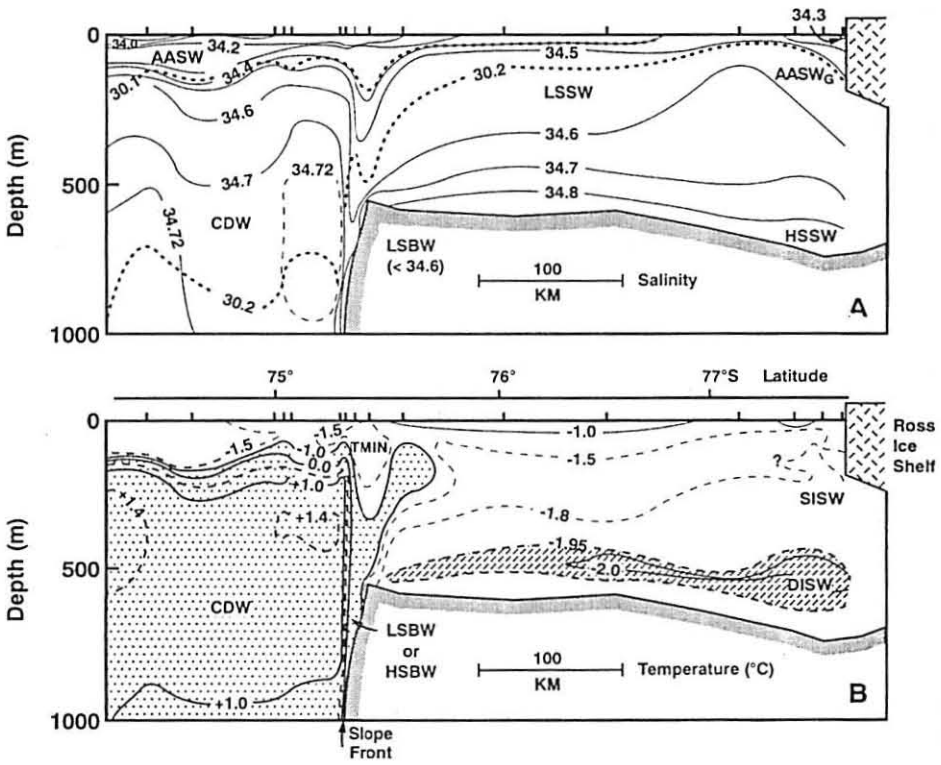

Fig. 35.13. Vertical sections of (*A*) salinity and (*B*) temperature that were obtained from a transect that extended from the Ross Ice Shelf to the outer shelf break in the Ross Sea. Station locations are indicated by the vertical tic marks. The dashed lines in the salinity section represent isopycnal surfaces referenced to 500 dB. (Adapted from Jacobs et al., 1985.)

the shelf margin. A recent analysis of the water-mass properties of the Antarctic shelf slope shows that the Antarctic Slope Front is present everywhere except in the Amundsen and Bellingshausen Seas (Kim, 1995). The analysis presented in Smith et al. (in press) also indicates the absence of the Antarctic Slope Front at the shelf edge on the contiental shelf west of the Antarctic Peninsula. These are regions in which meridional gradients in water mass properties are small and are characterized by the absence of dense water. The implication of an absent Antarctic Slope Front is that there is little or no flow to the west along the outer shelf in these regions.

The schematic circulation for the Antarctic Peninsula-Bransfield Strait suggests that the along- and across-shelf flows are not coherent over large distances. Rather, the shelf circulation seems to be composed of localized gyres with length scales that appear to be dictated by the rugged bottom topography. Similar mesoscale structure may be associated with the circulation on the Antarctic continental shelf in other regions; however, the data available are not adequate to resolve these flows.

The small internal Rossby radius of deformation associated with the Antarctic continental shelf (10–15 km) implies narrow currents. Hence coherent flows may exist, but sampling to date has been on scales too coarse to resolve these features. Also, the small coherence scale for the circulation suggests that small eddies should

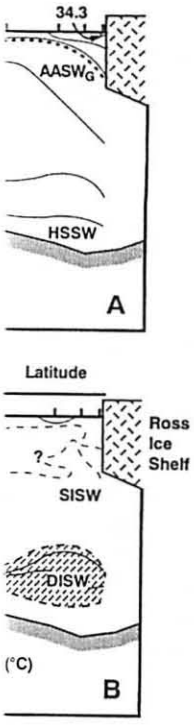

l from a transect that
ıcations are indicated
ıl surfaces referenced

of the Antarctic
ere except in the
ented in Smith et
at the shelf edge
regions in which
racterized by the
ope Front is that
egions.
l Strait suggests
listances. Rather,
ength scales that
soscale structure
al shelf in other
se flows.
th the Antarctic
erent flows may
e these features.
ıll eddies should

also be present. Some evidence for eddies on the Antarctic continental shelf exists (e.g., Heywood and Priddle, 1987), and some of these features may be permanent deflections of the flow (Stein, 1988).

The Polar Slope Current to the north of the South Shetland Islands is an example of the small scale nature of the coastal currents in the Antarctic. Describing the current required sampling at scales of less than 1 km (Nowlin and Zenk, 1988). It has been suggested that the Polar Slope Current to the north of the South Shetland Islands is continuous around Antarctica (Nowlin and Zenk, 1988). However, the simulated circulation from Capella (1989) suggests that this current does not extend west beyond the gap between Smith and Snow Islands. Recent XBT and CTD measurements made along transects that crossed the shelf break north of Livingston Island and west of Smith Island (Hofmann et al., 1993) support the suggestion that the Polar Slope Current is not continuous, as does the water-mass analysis presented by Kim (1995). However, these studies are not sufficient to determine the fate of this current.

8. Summary

CDW and its modified version, mCDW, play a major role in structuring the hydrographic characteristics of the Antarctic continental shelf from 150°E eastward to the Greenwich Meridian. The presence of this warm, salty water mass is necessary for bottom water formation to occur, and it has a profound effect on heat and salt budgets of Antarctic coastal waters. Moreover, the upward heat flux produced by mixing of CDW and resultant sea ice melt may moderate the amount of ice cover, as well as the climate, in Antarctic coastal regions. Hence small changes in the heat or salt content of CDW could result in climate changes in the Antarctic. MacAyeal (1985) suggests that entrainment-driven melting of the ice shelves in the Ross Sea could occur at depths shallower than 500 m if the ambient water column was warmed by 0.6°C. This would require that the warm-core water derived from the offshore CDW increase in temperature. Additionally, CDW and mCDW are high in nutrients, which when upwelled should produce enhanced primary production and increased phytoplankton biomass, assuming that other factors are not limiting. Thus localized upwelling of CDW and mCDW could provide predictable regions of increased food and possibly open water for the top predator populations that inhabit Antarctic coastal waters.

Coastal polynyas are an important aspect of the oceanography of the Antarctic continental shelf. The majority of the coastal polynyas are of the latent heat type and exist due to a balance between offshore transport of new sea ice and the seawater freezing rate. Under conditions of climate warming, the potential exists for changes in the size and frequency of occurrence of Antarctic coastal polynyas. If cooling over the Antarctic continent is reduced, the strength of the katabatic winds draining from the continent will be reduced, leading to a decreased export of ice from the coast and smaller (or vanishing) polynyas. Reduced polar cooling will also result in warmer air over the polynya and a decreased sea ice production rate, which can produce larger polynyas (see the length scale from Pease, 1987). Polynyas have the effect of concentrating brine production in a limited region, causing relatively large, but localized, changes in salinity. Spreading the sea ice formation over a larger area will result in an overall smaller salinity change. Thus, if the salt flux is reduced sufficiently, the brine will not be dense enough to penetrate into the deep ocean and will, instead, remain in

the surface layer. This change will result in widespread small changes of the surface salinity instead of larger but concentrated changes in the salinity of deeper water on the shelf. Thus climate change may result in a significant change in the production rate of Antarctic Bottom Water, which could potentially affect the larger-scale ocean circulation.

Thermodynamics are a critical component of physical processes on the Antarctic continental shelf. Where lower-latitude continental shelves are driven by coastal runoff or balanced buoyancy fluxes, high-latitude continental shelves must cope with extensive salt fluxes during the seasonal freeze–melt cycle of sea ice over the entire sea surface. Furthermore, the long periods of cooling and heating, driven by seasonal variations in sunlight, provide substantial thermohaline forcing, which drives vigorous circulation. The relatively thick layer of water on the shelf means that water retains much of its oceanic character near the bottom and is changed seasonally near the surface. Such vertical contrasts do not exist on shallower continental shelves, whatever the surface forcing. A further unique feature is the thick ice shelves covering some of the Antarctic continental shelf. The buoyancy-driven flow from these features may effectively convert warm salty water from lower depths on the shelf to fresher, colder water near the surface. Thus, understanding of the thermodynamic forcing of the Antarctic coastal waters is critical to development of circulation models and for understanding how this system may change with changing climate conditions.

The bottom topography of the Antarctic continental shelf is rugged and the limited measurements indicate that it exerts a strong effect on the circulation over the shelf. The dynamical scales of flow over the continental shelf are small, being on the order of 10–20 km, which is of the same order as many of the topographic features. Moreover, isolated depressions on the Antarctic continental shelf provide reservoirs for dense water, which may be released from the shelf by episodic mixing events. Across-shelf trenches 500–700 m in depth extend to the shelf break and thus provide conduits for the exchange of water between the continental shelf and the ocean. To date, little study has been made of the role of the rugged topography and small-scale bathymetric features on controlling circulation on the Antarctic continental shelf. Thus, advancing the understanding of the dynamics underlying the circulation on the Antarctic continental shelf will require sampling programs that are designed to capture the small but important scales associated with the dynamics.

Few of the historical hydrographic data were from studies dedicated specifically to mapping physical properties and circulation in Antarctic coastal waters. In fact, much of the existing data were obtained from multidisciplinary programs designed for biological sampling, and as a result the spatial resolution was not optimal for resolving hydrographic and circulation features. Observations on the inner shelf and during the austral winter were essentially lacking in most regions. Direct current measurements were even more limited, and most were confined to small regions of the outer shelf or to areas around ice shelves. Although useful, these measurements provide primarily representations of the locally driven circulation and do not provide a description of the large-scale flow on the continental shelf. Future sampling efforts in Antarctic coastal waters must be designed from the outset for physical oceanographic studies and should include high-resolution measurements, all seasons and the entire water column. The existence of such a database will greatly facilitate the development of theoretical models that are necessary for understanding the processes that underlie the circulation in Antarctic coastal waters.

Acknowledgments

This research was supported by the U.S. National Science Foundation, Office of Polar Programs by grant DPP-90-11927. Computer facilities and support were provided by the Commonwealth Center for Coastal Physical Oceanography at Old Dominion University. We thank R. Locarnini for constructive comments on an earlier version of this chapter and J. Morgan for invaluable assistance in editing the chapter.

References

Ainley, D. and S. S. Jacobs, 1981. Sea-bird affinities for ocean and ice boundaries in the antarctic. *Deep-Sea Res.*, **28,** 1173–1185.

Amos, A. F., 1993. RACER: the tides at Palmer Station. *Antarct. J. U.S.*, **28,** 162–164.

Amos, A. F., S. S. Jacobs and J.-H. Hu, 1990. RACER: hydrography of the surface waters during the spring bloom in the Gerlache Strait. *Antarct. J. U.S.*, **25,** 131–134.

Anon., 1991. Weather at U.S. stations, *Antarct. J. U.S.*, **26**(4), 23.

Anon., 1992. Weather at U.S. stations, *Antarct. J. U.S.*, **27**(4), 23.

Anon., 1993. Weather at U.S. stations, *Antarct. J. U.S.*, **28**(4), 23.

Bromwich, D. H. and D. D. Kurtz, 1984. Katabatic wind forcing of the Terra Nova Bay Polynya. *J. Geophys. Res.*, **89,** 3561–3572.

Bromwich, D. H. and C. R. Stearns, eds., 1993. *Antarctic Meteorology and Climatology: Studies Based on Automatic Weather Stations.* Antarctic Research Series, Vol. 61. American Geophysical Union, Washington, D.C.

Callahan, J. E., 1972. The structure and circulation of deep water in the Antarctic. *Deep-Sea Res.*, **19,** 563–575.

Capella, J. E., 1989. Circulation and temperature effects on the development and distribution of the eggs and larvae of the Antarctic krill, *Euphausia superba*: a modeling study. Ph.D. dissertation, Texas A&M University, College Station, Texas.

Capella, J. E., L. B. Quetin, E. E. Hofmann and R. M. Ross. 1992a. Models of the early life history of *Euphausia superba*. II. Lagrangian calculations. *Deep-Sea Res.*, **39,** 1201–1220.

Capella, J. E., R. M. Ross, L. B. Quetin and E. E. Hofmann, 1992b. A note on the thermal structure of the upper ocean in the Bransfield Strait–South Shetland Islands region. *Deep-Sea Res.*, **39,** 1221–1229.

Carmack, E. C., 1977. Water characteristics of the Southern Ocean south of the Polar Front. In *A Voyage of Discovery*, M. Angel, ed. G. Deacon 70th Anniversary Volume, *Deep-Sea Res.* (Suppl.). Pergamon Press, Elmsford, N.Y. pp. 15–42.

Carmack, E. C., 1990. Large-scale physical oceanography of polar oceans. In *Polar Oceanography, Part A: Physical Science*, W. O. Smith, Jr., ed. Academic Press, San Diego, Calif., pp. 171–222.

Carmack, E. C. and T. D. Foster, 1975. Circulation and distribution of oceanographic properties near the Filchner Ice Shelf. *Deep-Sea Res.*, **22,** 77–90.

Cavalieri, D. J. and S. Martin, 1985. A passive microwave study of polynyas along the Antarctic Wilkes Land coast. In *Oceanology of the Antarctic Continental Shelf*, S. S. Jacobs, ed. Antarctic Research Series, Vol. 43. American Geophysical Union, Washington, D.C., pp. 227–252.

Chelton, D. B., A. M. Mestas-Nuñez and M. H. Freilich, 1990. Global wind stress and Sverdrup circulation from the SEASat scatterometer. *J. Phys. oceanogr.*, **20,** 1175–1205.

Clowes, A. I. J., 1934. Hydrography of the Bransfield Strait. *Discovery Rep.*, **9,** 1–64.

Comiso, J. C. and A. L. Gordon, 1996. Cosmonaut polynya in the Southern Ocean: structure and variability. *J. Geophys. Res.*, **101,** 18,297–18,313.

Darby, M. S., A. J. Willmott and T. A. Somerville, 1995. On the influence of coastline orientation on the steady state width of a latent heat polynya. *J. Geophys. Res.*, **100,** 13625–13633.

Deacon, G. E. R., 1937. The hydrology of the Southern Ocean. *Discovery Rep.*, **15,** 1–124.

DeMaster, D. J., R. B. Dunbar, L. I. Gordon, A. R. Leventer, J. M. Morrison, D. M. Nelson, C. A. Nittrouer and W. O. Smith, Jr., 1991. Cycling and accumulation of biogenic silica and organic matter in high-latitude environments: the Ross Sea. *Oceanography*, **5,** 146–153.

Domack, E. W. and C. R. Williams, 1990. Fine structure and suspended sediment transport in three Antarctic fjords. In *Contributions to Antarctic Research I*, C. R. Bentley, ed. Antarctic Research Series, Vol. 50. American Geophysical Union, Washington, D.C., pp. 71–89.

Dunbar, R. B. and A. Leventer, 1991. Circulation in eastern McMurdo Sound, Antarctica, January through November 1990. *Antarct. J. U.S.*, **26**(5), 117–120.

Egbert, G. D., A. F. Bennett and M. G. G. Foreman, 1994. Topex/Poseidon tides estimated using a global inverse model. *J. Geophys. Res.*, **99,** 24,821–24,852.

Eicken, H. and H. A. Lange, 1989. Development and properties of sea ice in the coastal regime of southeastern Weddell Sea. *J. Geophys. Res.*, **94,** 8193–8206.

El-Sayed, S. Z., 1994. *Southern Ocean Ecology: The BIOMASS Perspective*. Cambridge University Press, Cambridge.

Fogg, G. E., 1992. *A History of Antarctic Science*. Cambridge University Press, Cambridge.

Foldvik, A., T. Gammelsrod and T. Torresen, 1985a. Circulation and water masses on the southern Weddell Sea shelf. In *Oceanology of the Antarctic Continental Shelf*, S. S. Jacobs, ed. Antarctic Research Series, Vol. 43. American Geophysical Union, Washington, D.C., pp. 5–20.

Foldvik, A., T. Kvinge and T. Torresen, 1985b. Bottom currents near the continental shelf break in the Weddell Sea. In *Oceanology of the Antarctic Continental Shelf*, S. S. Jacobs, ed. Antarctic Research Series, Vol. 43. American Geophysical Union, Washington, D.C., pp. 21–34.

Foster, T. D., 1972. Haline convection in leads and polynyas. *J. Phys. Oceanogr.*, **2,** 462–469.

Foster, T. D. and E. C. Carmack, 1976. Frontal zone mixing and Antarctic Bottom Water formation in the southern Weddell Sea. *Deep-Sea Res.*, **23,** 301–317.

FRAM Group, 1991. An eddy-resolving model of the Southern Ocean. *Eos*, **72**(169), 174–175.

Fraser, W. R., W. Z. Trivelpiece, D. G. Ainley and S. G. Trivelpiece, 1992. Increases in Antarctic penguin populations: reduced competition with whales or a loss of sea ice due to environmental warming? *Polar Biol.*, **11,** 525–531.

Gill, A. E., 1973. Circulation and bottom water production in the Weddell Sea. *Deep-Sea Res.*, **20,** 111–140.

Gloersen, P., W. J. Campbell, D. J. Cavalieri, J. C. Comiso, C. L. Parkinson and H. J. Zwally, 1992. *Arctic and Antarctic Sea Ice, 1978–1987: Satellite Passive-Microwave Observations and Analysis*. National Aeronautics and Space Administration, Washington, D.C.

Gordon, A. L., 1967. Structure of Antarctic waters between 20°W and 170°W. *Antarctic Map Folio Series*, folio 6, V. C. Bushnell, ed. American Geographyical Society, New York.

Gordon, A. L., 1981. Seasonality of Southern ocean sea ice. *J. Geophys. Res.*, **86,** 4193–4197.

Gordon, A. L. and E. J. Molinelli. 1982. *Southern Ocean Atlas*. Columbia Unviersity Press, New York.

Gordon, A. L. and W. D. Nowlin, Jr., 1978. The basin waters of the Bransfield Strait. *J. Phys. Oceanogr.*, **8,** 258–264.

Gordon, A. L. and P. Tchernia, 1972. Waters of the continental margin off Adélie Coast, Antarctica. In *Antarctic Oceanology II: The Australian–New Zeland Sector*, D. E. Hayes, eds., Vol. 19. American Geophysical Union, Washington, D.C., pp. 59–69.

Gordon, A. L., D. T. Georgi and H. W. Taylor, 1977. Antarctic Polar Front zone in the western Scotia Sea, summer 1975. *J. Phys. Oceanogr.*, **7,** 309–328.

Gordon, A. L., D. G. Martinson and H. W. Taylor, 1981. The wind-driven circulation in the Weddell-Enderby Basin. *Deep-Sea Res.*, **28,** 151–163.

Gordon, A. K., C. T. A. Chen and W. G. Metcalf, 1984. Winter mixed layer entrainment of Weddell Deep Water. *J. Geophys. Res.*, **89,** 637–640.

Grumbine, R. W., 1991. A model of the formation of high-salinity shelf water on polar continental shelves. *J. Geophys. Res.*, **96,** 22,049–22,062.

Hellerman, S. and M. Rosentein, 1983. Normal monthly wind stress over the world ocean with error estimates. *J. Phys. Oceanogr.*, **13,** 1093–1104.

Hellmer, H. H. and S. S. Jacobs, 1995. Seasonal circulation under the eastern Ross Ice Shelf, Antarctica. *J. Geophys. Res.*, **100,** 10,873–10,885.

Heywood, R. B. and J. Priddle, 1987. Retention of phytoplankton by an eddy. *Cont. Shelf Res.*, **7,** 937–955.

Hibler, W. D., III, 1979. A dynamic thermodynamic sea ice model. *J. Phys. Oceanogr.*, **9,** 815–846.

Hofmann, E. E., J. E. Capella, R. M. Ross and L. B. Quetin, 1992a. Models of the early life history of *Euphausia superba*. I. Temperature dependence during the descent–ascent cycle. *Deep-Sea Res.*, **39,** 911–941.

Hofmann, E. E., C. M. Lascara and J. M. Klinck, 1992b. Palmer LTER: upper ocean circulation in the LTER region from historical data. *Antarct. J. U.S.*, **27,** 239–241.

Hofmann, E. E., B. L. Lipphardt, Jr., D. A. Smith and R. A. Locarnini, 1993. Palmer LTER: hydrography in the LTER region. *Antarct. J. U.S.*, **28,** 209–211.

Hofmann, E. E., J. M. Klinck, C. M. Lascara and D. A. Smith, 1996. Water mass distribution and circulation west of the Antarctic Peninsula and including Bransfield Strait. In *Foundations for Ecological Research West of the Antarctic Peninsula*, R. M. Ross, E. E. Hofmann and L. B. Quetin, eds. Antarctic Research Series, Vol. 70. American Geophysical Union, Washington, D.C., pp. 61–80.

Jacobs, S. S., 1986. The antarctic Slope Front. *Antarct. J. U.S.*, **21,** 123–124.

Jacobs, S. S., 1991. On the nature and significance of the Antarctic Slope Front. *Mar. Chem.*, **35,** 9–24.

Jacobs, S. S. and J. C. Comiso, 1989. Sea ice and oceanic processes on the Ross Sea continental shelf. *J. Geophys. Res.*, **94,** 18,195–18,211.

Jacobs, S. S., A. F. Amos and P. M. Bruchhausen, 1970. Ross Sea oceanography and Antarctic Bottom Water formation. *Deep-Sea Res.*, **17,** 935–962.

Jacobs, S. S., R. G. Fairbanks and T. Horibe, 1985. Origin and evolution of water masses near the Antarctic continental margin: evidence from $H_2\,^{18}O/H_2\,^{16}O$ ratios in seawater. In *Oceanology of the Antarctic Continental Shelf*, S. S. Jacobs, ed. Antarctic Research Series, Vol. 43. American Geophysical Union, Washington, D.C., pp. 59–85.

Jaeger, J. M., C. A. Nittrouer, D. J. DeMaster, C. Kelchner and R. B. Dunbar. 1996. Lateral transport of settling particles in the Ross Sea and implications for the fate of biogenic material. *J. Geophys. Res.*, **101,** 18479–18488.

Jenkins, A. and C. S. M. Doake, 1991. Ice–ocean interaction on Ronne Ice Shelf, Antarctica, *J. Geophys. Res.*, **96,** 791–813.

Killworth, P. D., 1973. A two-dimensional model for the formation of Antarctic Bottom Water. *Deep-Sea Res.*, **20,** 941–971.

Killworth, P. D., 1974. A baroclinic model of motions on the Antarctic continental shelves. *Deep-Sea Res.*, **21,** 815–837.

Kim, S.-J., 1995. The transition zone between the oceanic and shelf regimes around Antarctica. M.S. thesis, Texas A&M University, College Station, Texas.

Klinck, J. M., 1995. Palmer LTER: comparison between a global tide model and observed tides at Palmer Station. *Antarct. J. U.S.*, **30**(5), 263–264.

Klinck, J. M., D. A. Smith and R. C. Smith, 1994. Hydrography in the LTER region during August and September 1993. *Antarct. J. U.S.*, **29,** 219–221.

Kock, K.-H. and M. Stein, 1978. Krill and hydrographic conditions off the Antarctic Peninsula. *Meeresforschung*, **26,** 79–95.

Kurtz, D. D. and D. H. Bromwich, 1985. A recurring, atmospherically forced polynya in Terra Nova Bay. In *Oceanology of the Antarctic Continental Shelf*, S. S. Jacobs, ed. Antarctic Research Series, Vol. 43. American Geophysical Union, Washington, D.C., pp. 177–201.

Large, W. G. and H. van Loon, 1989. Large scale, low frequency variability of the 1979 FGGE surface buoy drifts and winds over the Southern Hemisphere. *J. Phys. Oceanogr.*, **19,** 216–232.

Lemke, P., 1987. A coupled one-dimensional sea ice-ocean model. *J. Geophys. Res.*, **92,** 13,164–13,172.

Lemke, P., W. B. Owens and W. D. Hibler, III, 1990. A coupled sea ice-mixed layer-pycnocline model for the Weddell Sea. *J. Geophys. Res.*, **95,** 9513–9525.

Levitus, S. and T. Boyer, 1994a. *World Ocean Atlas 1994*, Vol. 2: *Oxygen*. NOAA Atlas NESDIS 2. U.S. Department of Commerce, Washington, D.C.

Levitus, S. and T. Boyer, 1994b. *World Ocean Atlas 1994*, Vol. 4: *Temperature*. NOAA Atlas NESDIS 4. U.S. Department of Commerce, Washington, D.C.

Levitus, S., R. Burgett and T. Boyer, 1994. *World Ocean Atlas 1994*, Vol. 3: *Salinity*. NOAA Atlas NESDIS 3. U.S. Department of Commerce, Washington, D.C.

Locarnini, R. A., 1994. Water masses and circulation in the Ross Gyre and environs. Ph.D. dissertation, Texas A&M University, College Station, Texas.

Lutjeharms, J. R. E., C. C. Stavropoulis and K. P. Koltermann, 1985. Tidal measurements along the Antarctic coastline. In *Oceanology of the Antarctic Continental Shelf*, S. S. Jacobs, ed. Antarctic Research Series, Vol. 43. American Geophysical Union, Washington, D.C., pp. 273–289.

MacAyeal, D. R., 1985. Evolution of tidally triggered meltwater plumes below ice shelves. In *Oceanology of the Antarctic Continental Shelf*, S. S. Jacobs, ed. Antarctic Research Series, Vol. 43. American Geophysical Union, Washington, D.C., pp. 133–143.

Middleton, J. H., T. D. Foster and A. Foldvik, 1982. Low-frequency currents and continental shelf waves in the southern Weddell Sea. *J. Phys. Oceanogr.*, **12,** 618–634.

Mosby, H., 1934. The waters of the Atlantic Antarctic Ocean. *Sci. Res. Norw. Antarct. Exped. 1927–1928*, **11,** 1–131.

Murphy, E. J., A. Clarke, C. Symon and J. Priddle, 1995. Temporal variation in Antarctic sea-ice: analysis of long term fast-ice record from the South Orkney Islands. *Deep-Sea Res.*, **42,** 1045–1062.

Neal, V. T. and W. D. Nowlin, Jr., 1979. International Southern Ocean studies of circumpolar dynamics. *Polar Rec.*, **19,** 461–471.

Nicolls, K. W. and A. Jenkins, 1993. Temperature and salinity beneath Ronne Ice Shelf, Antarctica. *J. Geophys. Res.*, **98,** 22,553–22,568.

Niiler, P., J. Illeman and J.-H. Hu, 1990. RACER: Lagrangian drifter observations of surface circulation in the Gerlache and Bransfield Straits. *Antarct. J. U.S.*, **25,** 134–137.

Niiler, P. P., A. Amos and J.-H. Hu, 1991. Water masses and 200 m relative geostrophic circulation in the western Bransfield Strait region. *Deep-Sea Res.*, **38,** 943–959.

Nittrouer, C. A., G. H. Pierson, J. M. Morrison and D. J. DeMaster, 1992. The movement of suspended materials in the Ross Sea. *Antarct. J. U.S.*, **27,** 77–79.

Nøst, O. A. and A. Foldvik, 1994. A model of ice shelf–ocean interactions with application to the Filchner-Ronne and Ross Ice Shelves. *J. Geophys. Res.*, **99,** 14243–14254.

Nowlin, W. D., Jr. and W. Zenk, 1988. Westward bottom currents along the margin of the South Shetland Island Arc. *Deep-Sea Res.*, **35,** 269–301.

Olbers, D., V. Gouretzki, G. Seib and J. Schroeter, 1992. *The Hydrographic Atlas of the Southern Ocean*. Alfred-Wegener-Institute for Polar and Marine Research, Bremerhaven, Germany.

Ou, H. W., 1988. A time dependent model of a coastal polynya. *J. Phys. Oceanogr.*, **18,** 584–590.

Owens, W. B. and P. Lemke, 1990. Sensitivity studies with a sea ice-mixed layer-pycnocline model in the Weddell Sea. *J. Geophys. Res.*, **95,** 9527–9538.

Parish, T. R. and D. H. Bromwich, 1987. The surface windfield over the Antarctic ice sheets. *Nature*, **328,** 51–54.

Pease, C. H., 1987. The size of wind-driven coastal polynyas. *J. Geophys. Res.*, **92,** 7049–7059.

Pillsbury, R. D. and S. S. Jacobs, 1985. Preliminary observations from long-term current meter moorings near the Ross Ice Shelf, Antarctica. In *Oceanology of the Antarctic Continental Shelf*, S. S. Jacobs, ed. Antarctic Research Series, Vol. 43. American Geophysical Union, Washington, D.C., pp. 87–107.

Potter, J. R. and J. G. Paren, 1985. Interaction between ice shelf and ocean in George VI Sound, Antarctica. In *Oceanology of the Antarctic Continental Shelf*, S. S. Jacobs, ed. Antarctic Research Series, Vol. 43. American Geophysical Union, Washington, D.C., pp. 35–58.

Quetin, L. B. and R. M. Ross, 1984. School composition of the Antarctic krill *Euphausia superba* in the waters west of the Antarctic Peninsula in the austral summer of 1982. *J. Crustacean Biol.*, **4,** 96–106.

Reid, J. L., W. D. Nowlin, Jr. and W. C. Patzert, 1977. On the characteristics and circulation of the southwestern Atlantic Ocean. *J. Phys. Oceanogr.*, **7,** 62–91.

Schumacher, J. D., K. Aagaard, C. H. Pease and R. B. Tripp, 1983. Effects of a shelf polynya on flow and water properties in the northern Bering Sea. *J. Geophys. Res.*, **88,** 2723–2732.

Schwerdtfegger, W. and L. R. Amaturo, 1979. Wind and weather around the Antarctic Peninsula. *Tech. Rep. 79.00.S1*. Department of Meteorology, University of Wisconsin, Madison, Wis.

Semtner, A. J., Jr., 1974. An oceanic general circulation model with bottom topography. Numerical simulation of weather and climate. *Tech. Rep. 9*. Department of Meteorology, University of California, Los Angeles.

Semtner, A. J., Jr. and R. M. Chervin, 1988. A simulation of the global ocean circulation with resolved eddies. *J. Geophys. Res.*, **93,** 15,502–15,522.

Semtner, A. J., Jr. and R. M. Chervin, 1992. Ocean general circulation from a global eddy-resolving model. *J. Geophys. Res.*, **97,** 5493–5550.

Sievers, H. A., 1982. Description of the physical oceanographic conditions, in support of the study on the distribution and behavior of krill. *Inst. Antart. Chil. Sci. Ser. 28*, pp. 73–122.

Sievers, H. A. and W. D. Nowlin, Jr., 1984. The stratification and water masses at Drake Passage. *J. Geophys. Res.*, **89,** 10,489–10,514.

Smith, N. and P. Tréguer, 1994. Physical and chemical oceanography in the vicinity of Prydz Bay, Antarctica. In *Southern Ocean Ecology: The BIOMASS Perspective*, S. Z. El-Sayed, ed. Cambridge University Press, Cambridge, pp. 25–43.

Smith, S. D., R. D. Muench and C. H. Pease, 1990. Polynyas and leads: an overview of physical processes and environment. *J. Geophys. Res.*, **95,** 9461–9479.

Smith, D. A., E. E. Hofmann, J. M. Klinck and C. M. Lascara, in press. Hydrography and circulation of the West Antarctic Peninsula continental shelf. *Deep-Sea Res.*

Smith, D. A., C. M. Lascara, J. M. Klinck, E. E. Hofmann and R. C. Smith, 1995. Palmer LTER: hydrography in the inner shelf region, *Antarct. J. U.S.*, **30**(5), 258–260.

Stammerjohn, S., 1993. Spatial and temporal variability in Southern Ocean sea ice coverage. M.S. thesis, University of California, Santa Barbara.

Stammerjohn, S. and R. C. Smith, 1996. Spatial and temporal variability in West Antarctic sea ice coverage. In *Foundations for Ecological Research West of the Antarctic Peninsula*, R. M. Ross, E. E. Hofmann and L. B. Quetin, eds. Antarctic Research Series, Vol. 70. American Geophysical Union, Washington, D.C., pp. 81–104.

Stein, M., 1981. Thermal structure of the Weddell-Scotia Confluence during February 1981. *Meeresforschung*, **29,** 47–52.

Stein, M., 1982. Fischereiozeanographische Untersuchungen während FIBEX 1981. *Arch. Fischereiwiss.*, **33,** 35–51.

Stein, M., 1983. The distribution of water masses in the South Shetland Islands area during FIBEX. *Mem. of Natl. Inst. Polar Res., Spec. Issue 27*, pp. 16–23.

Stein, M., 1986. Variability of water masses and currents off the Antarctic Peninsula during SIBEX. *Arch. Fischereiwiss.*, **37,** 25–50.

Stein, M., 1988. Variation of geostrophic circulation off the Antarctic Peninsula and in the southwest Scotia Sea, 1975–1985. In *Antarctic Ocean and Resources Variability*, D. Sahrhage, ed. Springer-Verlag, Berlin, pp. 81–91.

Stein, M., 1989. Seasonal variation of waters masses in Bransfield Strait and adjacent waters. *Arch. Fischereiwiss.*, **39,** 15–38.

Stein, M., 1992. Variability of local upwelling off the Antarctic Peninsula, 1986–1990. *Arch. Fischereiwiss.*, **41,** 131–158.

Stein, M. and R. B. Heywood, 1994. Antarctic environment–physical oceanography: The Antarctic Peninsula and Southwest Atlantic region of the Southern Ocean. In *Southern Ocean Ecology: The BIOMASS Perspective*, S. Z. El-Sayed, ed. Cambridge University Press, Cambridge, pp. 11–24.

Stein, M. and S. Rakusa-Suszczewski, 1983. Geostrophic currents in the South Shetland Islands area during FIBEX. *Mem. Nat. Inst. Polar Res. Spec. Issue 27*, pp. 24–34.

Stein, M. and S. Rakusa-Suszczewski, 1984. Meso-scale structure of water masses and bottom topography as the basis for krill distribution in the SE Bransfield Strait, February–March 1981. *Meeresforschung*, **30,** 73–81.

Stössel, A., P. Lemke and W. B. Owens, 1990. Coupled sea ice-mixed layer simulations for the Southern Ocean. *J. Geophys. Res.*, **95,** 9539–9555.

Toole, J. M., 1981. Sea ice, winter convection, and temperature minimum layer in the Southern Ocean. *J. Geophys. Res.*, **86,** 8037–8047.

Trenberth, K. E., J. G. Olson and W. G. Large, 1989. A global ocean wind stress climatology based on ECMWF analyses. *Tech. Note NCAR/TN-338+STR.*

Trenberth, K. E., W. G. Large and J. G. Olson, 1990. The mean annual cycle in the global ocean wind stress. *J. Phys. Oceanogr.*, **20,** 1742–1760.

van Loon, H., 1967. The half-yearly oscillations in the middle and high southern latitudes and the coreless winter. *J. Atmos. Sci.*, **24,** 472–486.

van Loon, H. and J. C. Rogers, 1984a. Interannual variations in the half-yearly cycle of pressure gradients and zonal wind at sea level on the Southern Hemisphere. *Tellus*, **35A,** 76–86.

van Loon, H. and J. C. Rogers, 1984b. The yearly wave in pressure and zonal geostrophic wind at sea level on the Southern Hemisphere and its interannual variability. *Tellus*, **36A,** 348–354.

Webb, D.J., P. D. Killworth, A. Coward and S. Thompson, 1991. *The FRAM Atlas of the Southern Ocean.* Natural Environmental Research Council, Swindon, Wiltshire, England.

White, W. B. and R. G. Peterson, 1996. An Antarctic circumpolar wave in surface pressure, wind, temperature and sea-ice extent. *Nature*, **380,** 699–702.

Whitworth, T., III and W. D. Nowlin, Jr., 1987. Water masses and currents of the Southern Ocean at the Greenwich Meridian. *J. Geophys. Res.*, **92,** 6462–6476.

Whitworth, T., III, W. D. Nowlin, Jr., A. H. Orsi, R. A. Locarnini and S. G. Smith, 1994. Weddell Sea Shelf water in the Bransfield Strait and Weddell-Scotia Confluence. *Deep-Sea Res.*, **41,** 629–641.

Zwally, H. J., J. C. Comiso and A. L. Gordon, 1985. Antarctic offshore leads and polynyas and oceanographic effects. In *Oceanology of the Antarctic Continental Shelf*, S. S. Jacobs, ed. Antarctic Research Series, Vol. 43. American Geophysical Union, Washington, D.C., pp. 202–226.